Author Manuscript

Author Manuscript

Author Manuscript

Author Manuscript

HHS Public Access

Author manuscript

Brain Behav Immun. Author manuscript; available in PMC 2024 June 13.

Published in final edited form as:

Brain Behav Immun. 2024 May ; 118: 1–21. doi:10.1016/j.bbi.2024.02.014.

Interferon-β deficiency alters brain response to chronic HIV-1 envelope protein exposure in a transgenic model of NeuroHIV

Hina Singh[1,2], **Jeffrey Koury**[1], **Ricky Maung**[1,2], **Amanda J. Roberts**[3], **Marcus Kaul**[1,2,*]

[1]Division of Biomedical Sciences, School of Medicine, University of California, Riverside, 900 University Ave, Riverside, CA, 92521, USA;

[2]Infection and Inflammatory Disease Center, Sanford Burnham Prebys Medical Discovery Institute, La Jolla, CA 92037, USA

[3]Animal Models Core, The Scripps Research Institute, 10550 North Torrey Pines Road, MB6, La Jolla, CA 92037, USA;

Abstract

Human immunodeficiency virus-1 (HIV-1) infects the central nervous system (CNS) and causes HIV-associated neurocognitive disorders (HAND) in about half of the population living with the virus despite combination anti-retroviral therapy (cART). HIV-1 activates the innate immune system, including the production of type 1 interferons (IFNs) α and β. Transgenic mice expressing HIV-1 envelope glycoprotein gp120 (HIVgp120tg) in the CNS develop memory impairment and share key neuropathological features and differential CNS gene expression with HIV patients, including the induction of IFN-stimulated genes (ISG). Here we show that knocking out IFNβ (IFNβKO) in HIVgp120tg and non-tg control mice impairs recognition and spatial memory, but does not affect anxiety-like behavior, locomotion, or vision. The neuropathology of HIVgp120tg is only moderately affected by the KO of IFNβ but in a sex-dependent fashion. Notably, in cerebral cortex of IFNβKO animals presynaptic terminals are reduced in males while neuronal dendrites are reduced in females. The IFNβKO results in the hippocampal CA1 region of both male and female HIVgp120tg mice in an ameliorated loss of neuronal presynaptic terminals but no protection of neuronal dendrites. Only female IFNβ-deficient HIVgp120tg mice display diminished microglial activation in cortex and hippocampus and increased astrocytosis in hippocampus compared to their IFNβ-expressing counterparts. RNA expression for some immune genes and ISGs is also affected in a sex-dependent way. The IFNβKO abrogates or diminishes the induction of MX1, DDX58, IRF7 and IRF9 in HIVgp120tg brains of both sexes. Expression analysis of neurotransmission related genes reveals an influence of IFNβ on multiple components with more pronounced changes in IFNβKO females. In contrast, the effects of IFNβKO on MAPK activities are independent of sex with pronounced reduction of active ERK1/2 but also of active p38 in the HIVgp120tg brain. In summary, our findings show that the absence of IFNβ impairs memory dependent behavior and modulates neuropathology in HIVgp120tg brains, indicating that

[*]**Corresponding author**: Marcus Kaul, Division of Biomedical Sciences, School of Medicine, University of California, Riverside, 900 University Ave, Riverside, CA, 92521, USA. marcus.kaul@medsch.ucr.edu.

Competing Interest

The authors declare no competing interest.

Author Manuscript Author Manuscript Author Manuscript Author Manuscript

its absence may facilitate development of HAND. Moreover, our data suggests that endogenous IFNβ plays a vital role in maintaining neuronal homeostasis and memory function.

Keywords

Interferon beta (IFNβ); IFNβ knockout; HIVgp120-transgenic; HIV associated neurocognitive disorder; behavior deficits; P38 MAPK; ERK1/2 signaling; Sexual dimorphism

1. Introduction

According to the World Health Organization (WHO) 38.4 million people were living with human immunodeficiency virus (HIV) worldwide as of 2021. Approximately 50% of people living with HIV develop HIV-associated neurocognitive disorder (HAND) in the combination anti-retroviral therapy era (Ojeda-Juarez et al., 2020; Saylor et al., 2016). Symptomatically, this disorder manifests as cognitive impairment, motor dysfunction and speech impairments; while neuropathologically, it is defined by synaptic degeneration and glial cell activation (Bell, 2004; Kaul et al., 2005; Ru and Tang, 2017; Thaney et al., 2017). Despite several decades of research, the cellular and molecular mechanisms involved in the pathogenesis of HAND remain only partially understood and no specific treatments are available (Singh et al., 2020; Thaney et al., 2017).

One model of brain injury inflicted by HIV infection is a HIVgp120 transgenic mouse (HIVgp120tg) expressing the viral gp120 envelope protein under the control of the glial fibrillary acidic protein (GFAP) promoter in astrocytes (Toggas et al., 1994). This model recapitulates key neuropathological features observed in human NeuroHIV patients, namely those with HIV encephalitis, including neuronal damage, astrocytosis, microgliosis, similar differential gene expression profiles and memory-related behavioral deficits (Maung et al., 2014; Ojeda-Juarez et al., 2020; Singh et al., 2020; Thaney et al., 2017). Employing the HIVgp120tg mice in previous studies we observed a crucial role of the innate immune system, specifically the type 1 interferon response, in promotion and amelioration of NeuroHIV (Maung et al., 2014). Type 1 interferons (IFNβ and IFNα) exert their biological function on the type 1 IFN receptor (IFNAR1/2 heterodimer), ultimately leading to activation of antiviral and neuroprotective components (Borden et al., 2007). In fact, we observed a transient increase of interferon beta (IFNβ), an anti-inflammatory and anti-viral type 1 interferon, preceding any behavioral or neuropathological signs in the HIVgp120tg mouse similar to what others observed in Simian Immunodeficiency Virus (SIV) models, suggesting a neuroprotective role for IFNβ in early HIV infection (Alammar et al., 2011; Thaney et al., 2017). To prolong the antiviral and potential neuroprotective effects of IFNβ on HIV induced neuronal damage, previous studies from our lab intranasally administered mouse recombinant IFNβ to HIVgp120tg mice resulting in neuroprotection mediated by IFNAR1 and CCL4 (Thaney et al., 2017). Later studies from our lab demonstrated that in the absence of neuroprotective amounts of exogenous IFNβ, IFNAR1 can contribute to neuronal injury in the presence of HIVgp120 in a sex dependent fashion (Singh et al., 2020), raising questions about the role of endogenous IFNβ in HIV induced neuronal injury.

Author Manuscript Author Manuscript Author Manuscript Author Manuscript

Hence, in the present study, we characterize the role of the endogenous ligand IFNβ in the HIVgp120tg mouse utilizing a global IFNβ knockout (IFNβKO) (Erlandsson et al., 1998).

We find that endogenous IFNβ is required to maintain neuronal homeostasis and memory function. However, genetic ablation of IFNβ also results in a partial reduction of HIV-induced injury, diminishing the loss of neuronal presynaptic terminals in CA1 of the hippocampus of both male and female mice. Interestingly, a reduction in microglial activation due to IFNβ knockout is only observed in cortex and hippocampus of females. The neurotransmission related gene expression and bioinformatics analysis further corroborates sexual dimorphism and alteration of comparably more components in females. In contrast, activities of mitogen-activated protein kinases (MAPK) and signal transducer and activator of transcription-3 (STAT3) are sex-independent. Altogether, the studies suggest a critical physiological and neuroprotective role of endogenous IFNβ in the brain which, however, is insufficient in the long-term to prevent neuronal injury caused by HIVgp120 exposure.

2. Materials and methods

2.1 Mouse models

HIVgp120tg mice expressing envelope glycoprotein gp120 of the HIV-1 strain LAV under the control of the GFAP promoter were kindly provided by Dr. Lennart Mucke (Gladstone Institute of Neurological Disease, University of California, San Francisco, CA) (Toggas et al., 1994) and previously used to study the role of CCR5 in NeuroHIV. Mice deficient in IFNβ (IFNβKO) were kindly provided by Dr. Tomas Leanderson (Lund University, Lund, SE) (Erlandsson et al., 1998). IFNβKO and HIVgp120tg mice were cross-bred, and the F3 generation of the HIVgp120tg^{het}- IFNβKO^{het} mice was used to obtain four genotypes, all on the C57BL/6.129/SJL background: (1) IFNβKO-HIVgp120 (KOGP; IFNβKO$^{-/-}$gp120^{+}), (2) HIVgp120 (GP; IFNβ$^{+/+}$gp120^{+}), (3) IFNβKO (KO; IFNβ$^{-/-}$gp120^{-}; control) and (4) wild-type (WT; IFNβ$^{+/+}$gp120^{-}, WT control). All procedures involving animals were performed in accordance and compliance with National Institute of Health *Guide for the Care and Use of Laboratory Animals* and approved by the Institutional Animal Care and Use Committees of the University of California, Riverside, Sanford-Burnham-Prebys Medical Discovery Institute and The Scripps Research Institute and this study follows the ARRIVE guidelines.

2.2 Behavioral testing

One cohort consisting of WT (male: 5, female: 7) HIVgp120tg (male: 5, female: 3), IFNβKO (male: 3, female: 6), and IFNβKO-HIVgp120 (male: 6, female: 7) mice were tested at 9–10 months of age by The Scripps Research Institute's (TSRI) Animal Models Core Facility. The behavioral tests were designed to examine cognitive abilities as well as other behaviors that could confound the interpretation of cognitive data, such as anxiety-like behavior, activity levels, and visual capability, and were performed in the following order: light/dark transfer (LDT), locomotor activity (LMA), optomotor (OM), novel object recognition (NOR), and Barnes maze test (BM). The behavioral tests were performed as previously published by our group (Hoefer et al., 2015; Maung et al., 2014; Ojeda-Juarez

Author Manuscript Author Manuscript Author Manuscript Author Manuscript

et al., 2020; Singh et al., 2020). The discrimination index for NOR was calculated using the formula, (time exploring the novel object – time exploring the familiar object) / (time exploring novel object + time exploring familiar object) * 100.

2.3 Immunohistology, quantitative fluorescence and deconvolution microscopy

Brain tissue harvest, immunofluorescence staining, deconvolution and quantitative fluorescence microscopy (neuronal injury and astrocytic activation) and cell counting (microglial activation) were performed as previously described (Hoefer et al., 2015; Maung et al., 2014; Singh et al., 2020; Thaney et al., 2017). Briefly, 9 to 10 months-old mice were terminally anesthetized with isoflurane and immediately transcardially perfused on ice through the left ventricle with 0.9% saline. The brain was subsequently removed and divided into two hemispheres, with one fixed in 4% paraformaldehyde (72h at 4°C) for histological analysis and the second dissected into hippocampus and cortex and subsequently snap frozen in liquid nitrogen for later RNA or protein extraction. Analysis of histopathology and RNA expression included 6 animals (3 females and 3 males) per group. For neuropathological assessment, 40 μm thick sagittal brain sections were prepared with a vibratome (Leica VT 1000S, Leica Biosystems, Buffalo Grove, IL) and immunostained using antibodies against synaptophysin (Syp; 1:50; Dako) and microtubule-associated protein 2 (MAP-2; 1:200; Sigma) as neuronal markers, or glial fibrillary acidic protein (GFAP; 1:250; Dako) and ionized calcium-binding adaptor molecule 1 (Iba1;1:125; Wako) as astrocytic and microglial markers, respectively. An Axiovert 200M fluorescence microscope (Carl Zeiss AG, Oberkochen, DE) with a motorized stage and Slidebook software (Intelligent Imaging Innovations version 6, Denver, CO) were used for image acquisition, deconvolution and quantitative analysis as recently published (Hoefer et al., 2015; Maung et al., 2014; Ojeda-Juarez et al., 2020; Singh et al., 2020; Thaney et al., 2017).

2.4 Isolation of mRNA and quantitative RT-PCR

Extraction, isolation and quantification of RNA of murine cerebral cortex and hippocampus was performed as previously described (Singh et al., 2020). Briefly, RNA of murine cerebral cortex and hippocampus was isolated using the Qiagen RNeasy Lipid Tissue Midi Kit (Qiagen, Cat# 75144) and Qiagen Mini Kit (Qiagen, Cat# 74104), respectively, according to the manufacturer's instructions. Quantitative RT-PCR (qRT-PCR) was performed as previously reported (Maung et al., 2014; Thaney et al., 2017). Firstly, RNA quality and concentration were determined using a NanoDrop DS-11 spectrophotometer (De Novix Inc., USA). 500ng of total RNA was reverse transcribed using SuperScript II reverse transcriptase (Invitrogen, USA) following the manufacturer's instructions. QRT-PCR was performed using 10μL of 2X Power PCR SYBR Green master mix (Applied Biosystems, USA), 1μL of cDNA (25ng), 8μL of PCR grade water and 0.5μL of forward and reverse primers. All qRT-PCR analysis was performed on the QuantStudio 6 flex Real-Time PCR System (Applied Biosystems/Thermo Fisher Scientific, Carlsbad, CA) using the following protocol: 95°C for 10 min, and for 40 cycles (95°C for 30s, 59°C for 1 min, 72°C for 1 min) followed by a denaturation step for melting temperature (Tm) analysis. The relative amount of mRNA of every gene *versus* the internal control (GAPDH) was calculated following the $2^{-\Delta\Delta Ct}$ method. The primer sequences are listed in Supplementary Table S1.

Author Manuscript Author Manuscript Author Manuscript Author Manuscript

2.5 GABA & Glutamate and Dopamine & Serotonin RT^2 Profiler™ PCR Array

Neurotransmission related gene expression analysis was performed using the GABA & Glutamate (PAMM-152Z) and Dopamine & Serotonin (PAMM-158Z) RT^2 Profiler™ Arrays following supplier's instructions (Qiagen, Germantown, MD). Previously isolated RNA, procedure described above, was reverse transcribed using the RT^2 First-Strand kit (Qiagen) mixed with RT^2 qPCR Master Mix containing SYBR Green (Qiagen). A QuantStudio™ 6 Flex System (Applied Biosystems/Thermo Fisher Scientific) was used to run all PCR arrays. The RT^2 Profiler™ Array Data Analysis software package (version 3.5) used the $2^{-(\Delta\Delta CT)}$-based method (Livak and Schmittgen, 2001) to calculate fold change and a modified Student's t-test to compute two-tail, equal variance *p*-values. This method calculates the difference between the gene of interest and the average of selected housekeeping genes (heat shock protein 90 alpha family class B member 1 (Hsp90ab1), Actin Beta (Actb), glyceraldehyde-3-phosphate dehydrogenase (Gapdh) and glucuronidase Beta (Gusb).

2.6 Ingenuity Pathway Analysis

Expression data for all 168 genes generated by RT^2 Profiler™ Arrays was further analyzed using Ingenuity Pathway Analysis (IPA; Ingenuity® Systems, www.ingenuity.com; build version: 486617M; content version: 46901286; release date: 2018–11-21) to generate the functional/biological gene networks. The IPA core analysis function was used and the same settings were employed as previously published with some minor changes in tissues and cell lines (inclusion of central nervous system cell line, immune cells and nervous system) (Singh et al., 2020).

2.7 Western blot analysis

Western blotting using lysates from mouse cortex and hippocampus was conducted as previously published with minor modifications (Medders et al., 2010; Singh et al., 2020). Briefly, dissected cortex or hippocampus was lysed on ice with 400–600μL of lysis buffer (10mL of 1X RIPA buffer, 100uL of phosphatase inhibitor (Calbiochem/EMD Chemicals, San Diego, CA) and one tablet of complete protease inhibitor (Roche; Indianapolis, IN)). Tissue was homogenized first with an electric pestle followed by trituration in a 3mL syringe. After adjusting of protein concentration based on results of the bicinchoninic acid (BCA) protein assay kit (Pierce/Thermo Fisher Scientific), 25–50μg of protein were added to 4X LDS sample buffer and 10X reducing agent (Invitrogen) and boiled for 5 min. Samples were loaded in a 4–12% SDS-PAGE gel (Invitrogen) and electrophoretically separated, and then electro-transferred to PVDF membranes. Afterwards, the membranes were blocked with 4% bovine serum albumin (BSA) in Tris-buffered saline containing Tween (TBS-T) and sub-sequentially incubated overnight at 4°C with the primary antibodies. Membranes were then washed with TBS-T and incubated with anti-mouse-HRP (AP128P; Millipore Sigma) and anti-rabbit-HRP (111-036-045; Jackson Immuno Reseach) secondary antibodies. Membranes were imaged using the ChemiDoc™ XRS+ imager (Bio-Rad Laboratories, Hercules, CA). Densitometry analysis was performed using ImageJ 1.52a software (http://rsb.info.nih.gov/nih-image/) and normalized against α-Tubulin or GAPDH expression levels. The following antibodies were used: phospho-p38 (1°Ab- 1:1000; Cell Signaling; 9211; anti-rabbit 2°Ab- 1:5000), total p38 (1°Ab- 1:2000; Cell Signaling;

Author Manuscript Author Manuscript Author Manuscript Author Manuscript

9212; anti-rabbit 2°Ab- 1:25,000), phospho-ERK1/2 (1°Ab- 1:1000; Cell Signaling; 9101S; anti-rabbit 2°Ab- 1:5000), total ERK1/2 (1°Ab- 1:2000; Cell Signaling; 9102; anti-rabbit 2°Ab- 1:5000), active JNK1/2 (1°Ab- 1:1000; Promega; V93A 20542917; anti-rabbit 2°Ab- 1:3000), total JNK1/2 (1°Ab- 1:1000; Cell Signaling; 9252; anti-rabbit 2°Ab- 1:3000), phospho-STAT1 serine 727 (1°Ab- 1:1000, Cell Signaling 8826; anti-rabbit 2°Ab- 1:3000), total STAT1 (1°Ab- 1:1000, Cell Signaling, 14994S; anti-rabbit 2°Ab- 1:3000), phospho-STAT3 tyrosine 705 (1°Ab- 1:1000; Cell Signaling; 9145; anti-rabbit 2°Ab- 1:5000), total STAT3 (1°Ab- 1:1000; Cell Signaling; 9139S; anti-mouse 2°Ab- 1:5000) and housekeeping genes α-tubulin (1°Ab- 1:2000; Sigma T9026; anti-mouse 2°Ab- 1:10,000) or GAPDH (1°Ab- 1:20,000; Ambion; 4300; anti-mouse 2°Ab- 1:25,000).

2.8 Statistical analysis

The analysis of histopathological data, mRNA expression and Western blotting data were performed using Graphpad Prism 8 software (GraphPad Software, Inc., CA, USA), behavioral data were evaluated using StatView (SAS Institute, Cary, NC). Comparisons of two groups were made by unpaired Student t-test, whereas multiple groups were compared using a single-step procedure for multiple comparisons with analysis of variance (ANOVA) followed by Fisher's protected least significant difference (PLSD) post hoc test (Lee and Lee, 2018). P-values < 0.05 were considered statistically significant. CT values were measured using RT^2 Profiler™ PCR Arrays. QIAGEN data analysis center (http://www.qiagen.com/geneglobe) was used for $2^{-(\Delta\Delta CT)}$-based fold change calculations and a modified Student's test to compute two tails, equal variance p-values. For the gene enrichment analysis right-tailed Fisher's exact test was performed.

3. Results

3.1 IFNβ is necessary for recognition memory and affects spatial learning

To investigate the effects of IFNβ on behavioral deficits associated with HIVgp120 expression in the brain, all four genotypes, WT; HIVgp120 (GP); IFNβKO (KO); and IFNβKO-HIVgp120 (KOGP), were subjected to behavioral testing at 9–10 months of age. There were no significant interactions between sex and genotype, therefore sexes were combined in the graphs. The LDT test showed no effects of HIVgp120 or IFNβ deficiency with or without gp120 on the time spent in the light compartment suggesting the absence of genotype-specific anxiety-like behavior (Fig. 1A). In the locomotor test there were no significant differences between genotypes in ambulation and rearing; however, HIVgp120 mice spent more time in the center of the arena relative to IFNβKO-HIVgp120 mice which suggests decreased anxiety-like behavior in the IFNβ-expressing mice (Fig. 1B). Indeed, while not significant, HIVgp120tg mice spent more time in the light compartment in the LDT test supporting this finding. There was no genotypic difference in head tracking behavior in the OPT test, signifying that the mice had intact vision (Supplementary Fig. S1). Overall, the results of these tests indicate that the mice are active, can see, and do not have impairments that would confound the results of the cognitive tests.

The NOR test was performed to assess short-term recognition memory. WT mice showed significantly more interest in the novel object than in the familiar object suggesting

Author Manuscript Author Manuscript Author Manuscript Author Manuscript

intact recognition memory. HIVgp120, IFNβKO and IFNβKO-HIVgp120 mice showed no significant differences in time spent with the familiar versus novel object, indicating impairment, and further suggesting a crucial role of IFNβ in recognition memory function (Fig. 1C). However, the NOR discrimination indices did not detect any significant differences between the four tested genotypes (Supplementary Fig. S2)

The BM test revealed no significant effects of genotype or sex on latency to escape and the numbers of errors made before escape across the training trials (Supplementary Fig S2). In the BM probe test in which the escape tunnel was removed so that spatial memory could be assessed, WT mice spent significantly more time in the target quadrant (where the escape tunnel had been) than the average of the other quadrants indicating intact spatial learning and memory. HIVgp120 expression and IFNβ deficiency each alone did not significantly affect spatial memory but the combination of the two (i.e. IFNβKO-HIVgp120 mice) completely disrupted spatial memory suggesting that the baseline level of IFNβ is pivotal for maintaining spatial cognition in mice chronically exposed to HIVgp120 (Fig. 1D).

3.2 IFNβ deficiency affects presynaptic terminals in HIVgp120tg and non-tg mice

Previous studies analyzing the cerebral cortex and hippocampus of HIVgp120tg mice have shown damage to presynaptic terminals. To characterize the role of IFNβ in this neuroHIV model, we harvested the brains of 9–10 months old mice and performed histopathological analysis. Quantification using deconvolution microscopy identified a significant loss of pre-synaptic terminals in HIVgp120 mice compared to WT controls in layer III of the cortex and CA1 region of hippocampus in both males and females (Fig. 2, Synaptophysin). IFNβ deficiency alone also resulted in the loss of SYP^+ neuropil in both the cortex and hippocampus of males while the females were unaffected, with no additional loss due to IFNβKO in cortex of HIVgp120 mice. However, IFNβKO in HIVgp120 mice partially diminished the loss of presynaptic terminals in hippocampus (CA1) of both the sexes (Fig. 2B & G).

3.3 IFNβ deficiency worsens loss of cerebrocortical neuronal dendrites in HIVgp120tg female mice

The HIVgp120 animals displayed a significant reduction in MAP2 fluorescence ($P < 0.0001$) in cortex and hippocampus (Fig. 2C & H, MAP2). IFNβ deficiency did not affect the $MAP2^+$ neurites in male cortex and hippocampus. In female cortex, IFNβKO animals showed significant loss ($P < 0.0001$) of neuronal dendrites compared to WT controls. The IFNβKO-HIVgp120 animals showed significant decrease in MAP2+ neurites compared to all the other three genotypes. The female hippocampus remained unaffected by the IFNβ deficiency in the absence of HIVgp120 (Fig. 2C & H).

3.4 IFNβKO does not prevent astrocytosis but diminishes microglial activation in females

Quantitative fluorescence analysis of the immunofluorescence-stained brain section for astrocytic GFAP showed a significant increase in both cerebral cortex and CA1 of the hippocampus in the presence of HIVgp120 compared to the WT controls (Fig. 2, GFAP). IFNβ deficiency did not alter the expression of GFAP in male and female cortex but did so in the female hippocampus. On the other hand, IFNβKO mice showed a trend to a

Author Manuscript Author Manuscript Author Manuscript Author Manuscript

higher baseline level of GFAP in the female hippocampus, which did not reach significance compared to the WT control. The IFNβKO-HIVgp120 mice showed a significant increase the GFAP level compared to HIVgp120 mice suggesting the IFNβ deficiency may perpetuate astrocytosis in female hippocampus while having no such effect in the cortex (Fig. 2D & I). IFNβ deficiency did not prevent nor did it worsen the microglia activation in the male cortex and hippocampus (Fig. 2, IBA1). On the other hand, the IFNβKO in HIVgp120 mice partially reduced microgliosis in the female cortex and hippocampus (Fig. 2E & J). However, the IFNβKO showed significant higher count for microglial cells in female cortex compared to the WT controls.

3.5 IFNβ deficiency affects expression of the viral transgene and host immune response-related genes

To assess the effects of IFNβ ablation on the expression of HIVgp120 envelope protein, we compared the mRNA levels in cerebral cortex and hippocampus. Analysis by qRT-PCR revealed that the IFNβKO-HIVgp120 genotype resulted in enhanced expression of gp120 mRNA as compared to HIVgp120 mice in male but not in female cortex (Fig. 3A). On the other hand, while there was a trend to decrease in the expression of gp120 mRNA in hippocampus of both males and females due to IFNβ deficiency, the difference was not significant (Fig. 3B). HIVgp120 expression in the brain, similar to HIV infection, is associated with enhanced expression of interferon-stimulated genes (ISGs), cytokines and chemokines (Maung et al., 2014; Singh et al., 2020; Thaney et al., 2017). Therefore, we next investigated expression levels of CCL4 and CCL5, two anti-viral genes implicated in neuroprotection (Cocchi et al., 1995). CCL4 was significantly upregulated in HIVgp120 mice compared to the WT controls in cortex and hippocampus of male and only in female cortex (Fig. 3C). The knockout of IFNβ resulted in no significant differences on the expression level of CCL4. However, in the female hippocampus there was no significant change in the CCL4 expression level between HIVgp120 mice and WT mice, but the knockout of IFNβ resulted in increased levels of CCL4 in IFNβKO-HIVgp120 mice compared to the other three genotypes (Fig. 3D). On the other hand, CCL5 levels were upregulated in HIVgp120 mice compared to the WT group; however, CCL5 expression was not changed by IFNβ deficiency in the cortex of males and females but the level of CCL5 in HIVgp120 and IFNβKO-HIVgp120 mice was higher in female cortex (Fig. 3E). In contrast, in male hippocampus IFNβKO-HIVgp120 mice showed significantly higher level of CCL5 compared to all the other three genotypes. Similarly, in female hippocampus the CCL5 level were upregulated in HIVgp120 compared to WT mice although not significantly and there was a trend increase in the level of CCL5 in IFNβKO-HIVgp120 mice compared to the other three genotypes (Fig. 3F).

We have previously shown that lipocalin-2 (LCN2) is one of the most up-regulated proteins in HIVgp120tg brains and contributes to neuronal damage and behavioral deficits in the HIVgp120 mice (Ojeda-Juarez et al., 2020). Unsurprisingly, qRT-PCR analysis showed the elevated level of LCN2 in these 9–10-month HIVgp120 brains compared to the WT control group in the cortex and hippocampus of males and females (Fig. 3G, H). The knockout of IFNβ in the HIVgp120 mice significantly increased the expression level of LCN2 compared to other three genotypes in male and female cortex and female hippocampus. But there

Author Manuscript Author Manuscript Author Manuscript Author Manuscript

was no significant effect of IFNβ deficiency on LCN2 level in the male hippocampus (Fig. 3H). The qRT-PCR results show that CCL2 expression was significantly upregulated in HIVgp120 mice in both the cortex and hippocampus of males and females (Fig. 4A & B). IFNβKO did not influence the expression of CCL2 in the cortex for both males and females, as well as in the female hippocampus. However, in the hippocampus, there was a significant decrease in the expression of CCL2 in IFNβKO-HIVgp120 mice compared to the HIVgp120 mice, but this effect was observed only in males. The expression of CCL3 is upregulated due to HIVgp120 in the cortex of males and females regardless of IFNβ genotype (Fig. 4C). No significant differences in CCL3 expression were observed among the four tested genotypes in the male hippocampus. However, in female hippocampus, the increase in CCL3 expression was not able to reach significance in the HIVgp120tg mice compared to the WT but knocking out IFNβ resulted in a significant increase in CCL3 in the IFNβKO x HIVgp120 mice compared to the other three genotypes (Fig. 4D).

Expression of MX1, an interferon induced GTP-binding protein, was significantly upregulated in the presence of HIVgp120 in the female cortex and hippocampus in both sexes. However, this increase was not statistically significant in male cortex. The baseline level of MX1 in HIVgp120tg controls was higher in female cortex and hippocampus (male and females) compared to the male cortex.(Fig. 4E & F). This upregulation of MX1 was absent in IFNβKO and IFNβKO-HIVgp120 mice, suggesting its increase to be completely dependent on this interferon. Like CCL2, CXCL10 has been implicated in HIV neuropathogenicity and higher expression levels of both CXCL10 and −11 were reported in the brain of HIVgp120 mice (Singh et al., 2020; Thaney et al., 2017). We observed significant upregulation in the expression of CXCL10 in HIVgp120 mice in both cortex and hippocampus consistent with our previous results (Ojeda-Juarez et al., 2020; Singh et al., 2020; Thaney et al., 2017). CXCL10 upregulation was not affected by the absence of IFNβ in both male and female cortex and in male hippocampus. However in female hippocampus, there was a significant decrease in the expression levels of CXCL10 in IFNβKO-HIVgp120 mice compared to the HIVgp120 mice.(Fig. 4G & H). Similarly, IFNβ deficiency did not affect the expression CXCL11 in male cortex while in female cortex there was a significant increase in the CXCL11 expression in IFNβKO-HIVgp120 mice compared to the HIVgp120 mice ($P < 0.05$)Fig. 4I). On the other hand, the mRNA expression of CXCL11 is not significantly different among the four tested genotypes in the hippocampus of either sex (Fig. 4J).The HIV-1 co-receptor CCR5 was also examined and the results revealed an upward trend of CCR5 levels associated with HIVgp120 in the cortex of both males and females, regardless of IFNβ, although the increase was not statistically significant in females(Fig. 4K). In the hippocampus, the RNA expression level of CCR5 was not significantly different between the four genotypes in either sex although, an increase associated with HIVgp120 was observed but without statistical significance due to variability (Fig. 4L). Additionally, STAT3 transcript levels were also assessed and showed that STAT3 expression was increased in the cortex and hippocampus of HIVgp120 mice. Specifically, in cortex, the expression of STAT3 was significantly higher in IFNβKO-HIVgp120 mice compared to HIVgp120 mice in both males and females ($P < 0.01$; $P < 0.05$) (Fig. 4M). However, in female hippocampus the levels of STAT3 significantly

Author Manuscript Author Manuscript Author Manuscript Author Manuscript

decreased after knocking out IFNβ in HIVgp120 mice, while the increase associated with HIVgp120 did not reach significance in IFNβ-deficient male hippocampus (Fig. 4N).

The comparably larger amounts of mRNA isolated from cortex allowed analyzing the mRNA expression levels of additional genes of the IFN system that have been implicated in HIV infection, namely DDX58 (RIG-I), IRF3, IRF7 and IRF9. HIV infection can activate the RIG-I signaling pathway which further leads to phosphorylation of IRF3 and IRF7 leading to production of type I IFNs (Berg et al., 2012; Singh et al., 2021). We observed an elevated mRNA expression level of DDX58, IRF3 ($P < 0.01$ in females only) and IRF7 in the HIVgp120 mouse cortex for both males and females. Compared to the HIVgp120 mice, the IFNβKO-gp120 mice exhibited a significant decrease in the expression level of DDX58 in males ($P < 0.001$) and females ($P < 0.0001$) (Fig. 5A). In male HIVgp120 mice there was only a trend to increase of IRF3 levels compared to wild-type controls, while in HIVgp120tg females IRF3 levels were significantly higher. Surprisingly, the absence of IFNβ did not have an impact on the mRNA expression level of IRF3 in either sex (Fig. 5B). In contrast, the absence of IFNβ resulted in a reduction of IRF7 expression in the HIVgp120 mice of both sexes. However, this decrease was more pronounced in females (Fig.5C). In males IRF7 still increased significantly in association with HIVgp120 when IFNβ was absent ($P < 0.05$).

IRF9 also plays an important role in activating the transcription of ISGs upon binding with STAT1-STAT2 heterodimer (Thaney and Kaul, 2019). Hence, we assessed the expression level of IRF9 in cortex. HIVgp120 mice displayed a significant upregulation of IRF9 in both males and females, compared non-tg genotypes. However, IFNβKO-HIVgp120 mice showed a significant lower induction of IRF9 compared to HIVgp120 mice in both males and females ($P < 0.05$; $P< 0.001$), although no significant difference was observed between WT control and IFNβKO mice (Fig. 5D).

3.6 Sex-dependent effects of IFNβ and HIVgp120 on neurotransmission-related gene networks

Next, we investigated whether the expression of genes involved in neurotransmission was affected by the deletion of the IFNβ gene in HIVgp120 brains. We used the RT2 Profiler™ PCR Arrays to analyze the GABA and glutamate (GG array: 84 genes) and dopamine and serotonin (DS array: 84 genes) neurotransmission systems and observed sex-dependent changes in expression of multiple neurotransmission related genes. The results indicated that when compared to their respective WT controls, the alterations in RNA expression in the cortex and hippocampus in association with HIVgp120 expression and the lack of IFNβ were greater in female than male mice. The results of the GABA and glutamate RT^2 Profiler PCR Arrays showed that in male cortex significant changes occurred in RNA expression of 15 genes while in female cortex of 26 genes (Fig. 6A & Supplementary Table S2). In the hippocampus, there were significant alteration in RNA expression level of 9 genes in males and 30 genes in females (Fig. 6B & Supplementary Table S3). The analysis of the dopamine and serotonin systems revealed in male cortex significantly altered RNA expression of 6 components as opposed to 27 components in females (Fig. 7A & Supplementary Table S4), while in the hippocampus 19 components were significantly altered in both males

Author Manuscript Author Manuscript Author Manuscript Author Manuscript

and females (Fig. 7B & Supplementary Table S5). The alteration of neurotransmission components from WT control differ in the presence of HIVgp120 with and without IFNβ and the IFNβKO itself, supporting the notion that IFNβ affects alone and in association with HIVgp120 neuronal integrity and behavioral performance. More pronounced changes in females are in line with our histological findings where we observed a more pronounced effect of IFNβKO in this sex.

Further, bioinformatics employing IPA enables the identification of functional gene networks and upstream regulators using the differential gene expression data for males and females generated with the RT2-arrays. Two high scoring networks were identified each in males and females: In male HIVgp120 cortex (score: 66; molecules involved 35); in female HIVgp120 cortex (score: 64; molecules involved 35) in male HIVgp120 hippocampus (score: 65; molecules involved 35) and female HIVgp120 hippocampus (score: 65; molecules involved 35). These networks are affected by IFNβ ablation and are shown in Fig 8 & 9 & Supplementary Table S6. Interestingly, CREB1 (cAMP response element binding protein-1), down-stream of p38 and ERK1/2 signaling (Koga et al., 2019), was seen downregulated in the male cortical and hippocampal networks due to IFNβKO and HIVgp120, but with no further change due to IFNβ ablation in cortex in the presence of HIVgp120. However, in the hippocampus only IFNβ deficiency alone leads to downregulation whereas HIVgp120 expression results in upregulation. In contrast, in females, CREB1 did not score high enough to be included in the top scoring networks of cortex or hippocampus. Notably, IPA also predicted CREB-binding protein (Cyclic adenosine monophosphate Response Element Binding Protein; CREBBP) as an upstream regulator in both cortex and hippocampus of males and females, which is in line with our previous work suggesting the involvement of CREB in HIVgp120 neurotoxicity (Singh et al., 2020). The complete list of upstream regulators and their Z-scores is shown in Supplementary Table S7.

3.7 IFNβ modulates the effects of HIVgp120 on MAPK activity

Activation of p38 MAPK has been implicated in neuronal death and macrophage/micro-glia activation in HIV neurotoxicity (Kaul and Lipton, 1999; Medders et al., 2010). Higher levels of phosphorylated p38 can be seen in cortex of HIVgp120 mice; however, we have reported earlier that the balance of all MAPK signaling is crucial to achieve complete neuroprotection in HIVgp120 mice (Ojeda-Juarez et al., 2020; Singh et al., 2020). To quantify active p38 MAPK, we performed Western blots for the phosphorylated kinase and its total protein. The immunoblotting results in the cortex revealed that there was a significant increase in the phospho-p38 level in HIVgp120 mice compared to the WT controls. This increase was absent in the IFNβKO-HIVgp120 mice suggesting that IFNβ deficiency permits neuronal injury without an increase and even at decreased levels of phosphorylated p38 in the cortex. We observed no sex differences and no significant difference in expression level of total p38 in any of the tested genotypes (Fig.10 A–D).

The involvement of ERK1/2 in HIV-associated neuronal injury is well characterized and we have shown earlier in 11–14 months old HIVgp120 mice that reduction of hippocampal phosphorylated ERK1/2 (pERK1/2/) was associated with neuronal damage (Mocchetti and

Author Manuscript Author Manuscript Author Manuscript Author Manuscript

Bachis, 2004; Singh et al., 2020). Therefore, pERK1/2 was also assessed and revealed that in the cortex there was a trend of an increase in the level of pERK1/2 in HIVgp120 mice compared to WT controls. However, IFNβ deficiency significantly reduced the level of pERK1/2 compared to the IFNβ-expressing genotypes and the decrease was consistent in IFNβKO-HIVgp120 mice, suggesting that IFNβ is crucial to maintain normal levels of pERK1/2. The involvement of ERK1/2 in HIV-associated neuronal injury is well characterized and we have shown earlier in 11–14 months old HIVgp120 mice that reduction of hippocampal phosphorylated ERK1/2 (pERK1/2/) was associated with neuronal damage (Mocchetti and Bachis, 2004; Singh et al., 2020). Therefore, pERK1/2 was also assessed and revealed that in the cortex there was a trend of an increase in the level of pERK1/2 in HIVgp120 mice compared to WT controls. However, IFNβ deficiency significantly reduced the level of pERK1/2 compared to the IFNβ-expressing genotypes and the decrease was consistent in IFNβKO-HIVgp120 mice, suggesting that IFNβ is crucial to maintain normal levels of pERK1/2. Total ERK1/2 expression remained relatively unchanged in all the tested genotypes except for a significant drop in total ERK1/2 in IFNβKO-HIVgp120 mice compared to the WT and HIVgp120 mice expressing IFNβ. While no change was observed for pERK1/2 in hippocampus of 9–10 months old HIVgp120 compared to WT mice, a significant reduction was observed in IFNβKO mice compared to the IFNβKO-HIVgp120 mice at this age. There were no sex differences and no significant changes in the expression of total ERK1/2 in any of the tested genotypes (Fig.10 E–H).

Next, levels of active and total cJun N-terminal kinase (JNK) 1/2 were assessed by western blotting. No significant changes were found for active JNK1/2 or total JNK1/2 in both cortex and hippocampus in HIVgp120 or IFNβKO genotypes, although average levels trended higher in cortex of IFNβKOs (Fig. 11 A–D).

Type 1 IFNs are one of the major player for activation of the Janus kinase-signal transducer and activator of transcription (JAK-STAT) pathway to activate ISGs (Doyle et al., 2015; Schoggins et al., 2011). HIVgp120 protein activates STAT1 in vitro, causing inflammation and blood brain barrier dysfunction (Yang et al., 2009), similarly we have reported higher level of STAT1 in brains of HIVgp120 mice (Singh et al., 2020).

Consequently, phosphorylated-STAT1 and STAT1 was investigated through Western blot, the pSTAT1 analysis in the cortex showed that HIVgp120tg mice had significantly higher levels of pSTAT1 when comparted to the other three genotypes and this elevation was absent the IFNβKO-HIVgp120 mice. The expression of STAT1 protein was significantly higher in HIVgp120 mice compared to all the tested genotypes. However, IFNβ deficiency is associated with a significantly reduced level at baseline when compared to the WT controls. On the other hand, in hippocampus, pSTAT1 trended slightly above the baseline level in the presence of HIVgp120 and IFNβ but without reaching significance (Fig. 12 A–D). Similarly, the total STAT1 expression was significantly increased in the HIVgp120 mice compared to all the other genotypes suggesting the absence of IFNβ signaling prevents an increase of pSTAT1 and STAT protein in both cortex and hippocampus.

STAT3 is one of the key factors promoting neuronal survival by inducing neuroprotective genes (Dziennis and Alkayed, 2008), therefore, we analyzed the levels STAT3 in cortex and

Author Manuscript Author Manuscript Author Manuscript Author Manuscript

hippocampus. In HIVgp120 mice, the levels of phosphorylated STAT3 were found to be significantly elevated when compared to the WT control group. The absence of IFNβ did not have any effect on the levels of pSTAT3. On the other hand, HIVgp120 mice exhibited a significant increase in the levels total STAT3, and the deletion of IFNβ did not affect these levels. In hippocampus, we observed an upregulation of pSTAT3 in the HIVgp120 mice, and even more so in IFNβKO-HIVgp120 mice (Fig. 12 E–H). The levels of total STAT3 were also elevated in the presence of HIVgp120, but IFNβ deficiency had no effect.

4. Discussion

Infection with HIV leads to the production of IFNs which have the ability to interfere with viral replication. IFNα and -β, constitute the type I IFNs and play a major role as the first line of host defense against HIV in the brain (Thaney and Kaul, 2019). We have shown previously that intranasal treatment with IFNβ prevents in vitro and in vivo neuronal damage triggered by HIVgp120, contingent on the presence of IFNAR1 and CCL4 (Thaney et al., 2017). However, in the absence of neuroprotective levels of IFNβ, IFNAR1 (the receptor for type I IFNs) can contribute to HIVgp120 induced neuronal injury and neurocognitive and memory impairment, presumably by permitting signaling of IFNα (Singh et al., 2020). The present study shows that the baseline level of IFNβ is crucial to maintaining normal neuronal function, while the knockout of IFNβ in HIVgp120 mice partially diminishes in a sex-dependent fashion some aspects of neuronal injury. One possible explanation is that IFNβKO also prevents regulation of factors that can contribute to neuronal injury, such as IFNα (Erlandsson et al., 1998).

Behavioral testing confirmed that 9–10 month-old HIVgp120 mice have impaired recognition memory while, in contrast to their 11–14 month-old counterparts (Singh et al., 2020), spatial memory is still functional if they express IFNβ. Our study also reveals that IFNβ deficiency itself can have a detrimental effect on these cognitive functions. Moreover, unlike our previous observation with 11–14 month-old HIVgp120tg mice, we did not find any sex-dependent differences in NOR and BM tests of the mice aged 9–10 months (Ojeda-Juarez et al., 2020; Singh et al., 2020). In this study only WT mice had intact recognition memory. Novel object recognition involves hippocampus and perirhinal cortex (Mumby et al., 2005; Winters et al., 2004). Therefore, the behavioral phenotype fits with the damage to $MAP2^+$ neurites and SYP^+ presynaptic terminals in cortex and hippocampus of both sexes. In contrast, the compromised recognition memory in IFNβ deficient mice is not entirely reflected by neuronal and synaptic injury since a reduction of neurites was only observed in the cortex of female IFNβKO mice and a loss of SYP^+ presynaptic terminals was only observed in the cortex and hippocampus of male IFNβKO mice. Moreover, the changes in IFNβKO were not as pronounced as seen in the HIVgp120 and IFNβKO-HIVgp120tg mice. The role of IFNβ in maintaining normal neurites and presynaptic terminals warrants further examination.

The BM test of spatial memory is sensitive to impaired hippocampal function (Paylor et al., 2001) and not significantly affected in the 9–10 month-old HIVgp120 and IFNβKO mice in contrast to the IFNβKO-HIVgp120 mice, suggesting that the combination of neurotoxic viral protein with lack of protective IFNβ worsens impairment of spatial learning. A

Author Manuscript Author Manuscript Author Manuscript Author Manuscript

possible explanation is the persistence of damage in hippocampal neuronal dendrites seen in HIVgp120 and IFNβKO-HIVgp120 mice while the ameliorated injury to SYP^+ presynaptic terminals associated by IFNβKO is not sufficient to protect the mice from impaired spatial learning. In fact, the IFNβ-expressing HIVgp120 mice perform comparably in the spatial memory task to their IFNβKO counterparts despite a more pronounced loss of SYP^+ presynaptic terminals. Thus, IFNβ may support spatial memory in an as yet uncharacterized fashion even if synapses are compromised. Alternatively, SYP^+ presynaptic terminals may not be functionally normal in the absence of IFNβ, which could explain the differences in the expression of multiple components of the here investigated four major neurotransmission systems.

In contrast to the behavioral assessments, the immunohistochemistry data shows pronounced sex- and brain region-dependent effects of IFNβ deficiency. The loss of presynaptic terminals in both cortex and hippocampus of males suggests that the baseline level of IFNβ is required to maintain neuronal homeostasis. On the other hand, no reduction of presynaptic terminals was observed in female cortex or hippocampus due to IFNβ deficiency. The diminished injury of SYP^+ presynaptic terminals was specific to the hippocampus of IFNβKO-HIVgp120 mice of both sexes. The decreasing trend in the expression level of HIVgp120 mRNA in the hippocampus of IFNβ-deficient males and females could explain, at least in part, the protection observed in the hippocampus. Our lab has previously observed that the effect of IFNAR1 on damage to SYP^+ presynaptic terminals varied by brain region and sex, and the hippocampus was more protected in females than males (Singh et al., 2020).

The other prominent pathological hallmarks of HIV brain pathology are astrocytosis and microgliosis (Ojeda-Juarez et al., 2020; Thaney et al., 2017). IFNβ ablation does not prevent astrocytosis induced by HIVgp120 in male and female cortex and male hippocampus, as judged by GFAP expression. This finding is in line with our previously published work (Singh et al., 2020). However, a significant increase in GFAP expression was observed in the female hippocampus of IFNβKO-HIVgp120tg mice, which indicates that IFNβ limits astrocytosis in a sex-dependent mechanism which warrants further investigation. On the other hand, IFNβ ablation ameliorated the HIVgp120 induced microgliosis in the both cortex and hippocampus of females but not males. The lower numbers of microglial cells in female hippocampus could also explain the protection observed for presynaptic terminals in female hippocampus, which is in line with our previous observation in CCR5-deficient HIVgp120 mice (Maung et al., 2014). On the other hand, the reduced numbers of microglia in female cortex were not sufficient to provide protection of presynaptic terminals, suggesting the involvement of an additional IFNβ-dependent mechanism that counteracts synaptic injury in the presence of microglial activation.

Our previous study has shown a sex effect on expression of viral envelope protein gp120 in the brain with an increase in males of IFNAR1-deficient mice (Singh et al., 2020). Here we investigated the RNA expression of HIVgp120 in both the brain regions and in line with the earlier observation, only male IFNβKO-HIVgp120 mice showed higher expression of HIVgp120, and only in cortex, suggesting a sex specific effect of the IFNα/β-IFNAR1 axis that warrants further study. The transgenic expression of viral envelope gp120 is also known

Author Manuscript Author Manuscript Author Manuscript Author Manuscript

to upregulate several other components of the innate immune response, such as CCL2, −3, −4, −5, CXCL10 and LCN2. The β-chemokines CCL3, −4 and −5 are natural ligands of HIV co-receptor CCR5 that suppress HIV-1 infection (Cocchi et al., 1995). In addition, we have shown that CCL4 and CCL5 can protect neurons from HIVgp120 induced neuronal injury (Kaul and Lipton, 1999; Thaney et al., 2017). Interestingly, IFNβ ablation affected the RNA expression level of CCL4 only in female hippocampus and that of CCL5 in male hippocampus of HIVgp120 mice revealing a sex effect on the expression of these antiviral and neuroprotective chemokines. Also, CCL3 was upregulated only in IFNβKO-HIVgp120 female hippocampus. Overall, upregulation of β chemokines only in the hippocampus may contribute to the partial protection observed for presynaptic terminals. In contrast, IFNβ deficiency does not affect the expression level of these β-chemokine in the cortex which in part can explain the lack of protection seen in the cortex. Strikingly the absence of IFNβ resulted in loss of presynaptic terminals in both brain regions in males and loss of $MAP2^+$ neurites only in female cortex, suggesting that a baseline amount of IFNβ is necessary to maintain neuronal homeostasis.

CCL2 is upregulated in HIVgp120 mice and while IFNβ ablation did not influence expression in male cortex, a significant downregulation occurred in the hippocampus of IFNβKO-HIVgp120 male mice. In the cortex and hippocampus of female, IFNβKO-HIVgp120 mice, there was a noticeable trend towards a reduction in expression of CCL2.. That finding may at least in part explain the lower microglial count observed in the female cortex and hippocampus. The protection of presynaptic terminals in the hippocampus but not in the cortex of IFNβKO-HIVgp120 animals is similar to our previous observations in IFNAR1KO mice, where we observed sexual dimorphism in CCL2 expression, suggesting that additional sex-dependent factors regulate CCL2 (Singh et al., 2020). CXCL10 has been implicated in HIV neuropathogenesis and our study indicated that the CXCL10 level remains unaffected by the absence of IFNβ, possibly contributing to the loss of $MAP2^+$ neurites in cortex and hippocampus (Sanders et al., 1998). However, a significant, albeit slight, decrease in CXCL10 levels was observed in female hippocampus in IFNBKO-HIVgp120 compared to HIVgp120 mice, which however was not sufficient to protect against damage to $MAP2^+$ neurites.

We have recently shown that exogenous, transnasally administered IFNβ can increase the expression level of CXCL11 in HIVgp120 brain and knocking out IFNAR1 can completely abrogate the chemokine's expression in the hippocampus, implicating the type I IFN response as a necessary component for regulation of CXCL11 (Singh et al., 2020; Thaney et al., 2017). Although knocking down IFNβ in HIVgp120 mice does not affect the expression level of CXCL11 in the male cortex or hippocampus of either sex, a noteworthy upregulation was observed in the female cortex of IFNβKO-HIVgp120 mice, suggesting an IFNβ-independent of type I IFN signaling. IFNα may continue to signal through the IFNAR1 receptor and could be an inducer of CXCL11 production. In the cortex, the absence of IFNβ inhibits the HIVgp120-triggered expression of MX1, DDX58, IRF7, and IRF9 at the RNA level, indicating it requires IFN signaling and IRF7 seems most dependent on IFNβ signaling. In contrast, the lack of IFNβ does not impact the mRNA level of IRF3, indicating that other factors can increase its expression in HIVgp120 mice in a sex-dependent manner. The RNA induction of MX1, RIG-I, IRF7 and IRF9, which is

Author Manuscript Author Manuscript Author Manuscript Author Manuscript

responsible for the anti-viral state induced by type I IFNs, and protein level of STAT1, which is responsible for JAK/STAT signaling to activate ISGs, all were abrogated in HIVgp120 mice lacking IFNβ. This suggests that the type I IFN response to the viral trigger but not the baseline expression is abolished in both brain structures following ablation of IFNβ (Doyle et al., 2015; Singh et al., 2020; Thaney et al., 2017). On the other hand, the pSTAT3 expression and STAT3 transcript either trends towards or is significantly upregulated in the cortex of IFNβKO-HIVgp120 compared to the HIVgp120 animals. STAT3 in the CNS is implicated in shunting neuronal progenitors away from differentiating into neurons and more preferentially into astrocytes, thus providing a possible explanation for astrocytosis (Li et al., 2021). However, the absence of IFNβ did not result in any notable changes in protein levels of phospho STAT3 and total STAT3 in the cortex. These findings do not exclude that IFNβ may play a role in regulating STAT3 expression in the brain in the context of HIV infection but show that IFNβ is not required for increasing STAT3 levels. Further research is needed to fully elucidate the mechanisms governing STAT3 function in the brain in the presence and absence of HIV.

We recently showed a role for LCN2 in behavioral impairment, neuronal damage and microglia activation in HIVgp120 mice (Ojeda-Juarez et al., 2020). Here, we observed an increase in the transcript level of LCN2 in cortex of IFNβKO-HIVgp120 mice and in female hippocampus, which provides a potential, additional explanation for neuronal injury associated with a more pronounced behavioral deterioration compared to the other genotypes.

Expression of genes related to neurotransmission is also affected by IFNβ-deficiency in a sex-dependent fashion in both cortex and hippocampus. HIVgp120 and IFNβKO with and without gp120 altered the different components of GABAergic, glutaminergic, dopaminergic, and serotonergic neurotransmission systems compared to WT controls. Notably, females displayed alteration of more pre- and post- synaptic components in comparison to males in both cortex and hippocampus suggesting a more pronounced effect of endogenous IFNβ in females. While sexual dimorphism in the components of neurotransmission systems is in line with our earlier studies (Ojeda-Juarez et al., 2020; Singh et al., 2020), it is the first time we observe more pronounced changes in females. Subjecting the gene expression data to IPA, we identified sex differences in top gene networks that are affected by HIVgp120 and IFNβ deficiency in cortex and hippocampus. Interestingly, CREB1 scored high enough to be included in the networks for cortex and hippocampus of males but not females. However, IPA predicted CREB binding protein (CREBP) as the major upstream regulator in cortex and hippocampus of both sexes, which is in line with our studies on the role of IFNAR1 suggesting the involvement of CREB1 in the IFN response (Singh et al., 2020). In a separate earlier study, we observed a network linking CREB1 and p38MAPK, and CREB1 is known to be regulated by p38MAPK and ERK1/2 (Ojeda-Juarez et al., 2020). Here we show the sex-independent effect of MAPK signaling and the increase of phospho-p38 in cortex of HIVgp120tg brain corresponding with neuronal injury, while downregulation of p38 activity in the IFNβKO mice appears insufficient to provide neuronal protection. The persistent neuronal damage may be explained by the concomitant inhibition of phosphorylated and total ERK1/2 signaling in the cortex of IFNβ deficient mice with and without HIVgp120. We and others have shown previously

Author Manuscript Author Manuscript Author Manuscript Author Manuscript

that activation of ERK1/2 is one of the key signaling pathways contributing to neuronal protection (Mocchetti and Bachis, 2004; Singh et al., 2020). In contrast, active and total p38 levels remain unchanged in the hippocampus of HIVgp120 and IFNβKO mice, a finding in line with our earlier study of the role of IFNAR1 (Singh et al., 2020). Thus, the diminished injury seen in the hippocampal pre-synaptic terminals of IFNβKO-HIVgp120 mice might result from increased ERK1/2 signaling. On the other hand, the downregulation of active ERK1/2 in the IFNβKO mice below the baseline level may explain the pre-synaptic terminal damage seen in male IFNβKO hippocampus. The dysregulation of MAPK singling pathways in neurocognitive disorders is widely recognized (Kim and Choi, 2010) and our data support the notion IFNβ affects the balance of all MAPK signaling that is vital to achieve neuroprotection.

A study conducted with macaques has demonstrated that IFNβ can inhibit the continued replication of SIV within macrophages, indicating that IFNβ may be able to regulate SIV replication within the CNS (Barber et al., 2004). Additionally, IFNβ was shown to prevent HIV-1 infection in primary cultures of human fetal microglia as well as production of chemokines CCL3, CCL4, and CCL5 (Kitai et al., 2000). Minagawa et al. (1989), reported high levels of human IFNβ in the sera of HIV-1 infected patient, especially asymptomatic carriers (Minagawa et al., 1989). Another study has shown increased IFNβ gene expression in the gut, but not in blood, in persons with HIV-1 infection compared to age/gender-matched uninfected controls (Le Dreau et al., 1998). These reports suggest that the IFN response might differ in various parts of the body during chronic HIV-1 infection. Surprisingly, existing literature on IFNβ signaling in people living with HIV (PLWH) with HAND/HAD is very limited and more research is needed to clarify the specific impact of IFNβ signaling on neurocognition of PLWH.

On the other hand, the levels of IFN-α in the cerebrospinal fluid are higher in individuals with HAD compared to those without HAD (Krivine et al., 1999; Perrella et al., 2001; Rho et al., 1995). Recent research has shown that both type I and type II interferon response genes are activated in the brains of HIV patients without neurocognitive impairment, as well as in HIV patients with HIV encephalitis (HIVE), particularly in white matter, frontal cortex, and basal ganglia (Gelman et al., 2012; Sanna et al., 2017). The earlier study reported that genes related to the IFN response, such as CD163 (cluster of differentiation 163), PSMB8 (proteosome subunit beta type 8), GBP1 (guanylate binding protein 1) and BTN3A3 (butyrophilin subfamily 3 member A3) were significantly upregulated in the white matter, frontal cortex and basal ganglia of HIV infected individual with neurocognitive impairment with HIVE compared to those without neurocognitive impairment (Gelman et al., 2012). The latter study found that HIV patients with neurocognitive impairment but without HIVE did not show activation of IFNs but they did have increased expression of chemokines, cytokines and β-defensins in the white matter (Sanna et al., 2017). These findings indicate complex interaction between IFN response, neurocognitive impairment and HIV infection which warrants further research.

The present study has a limitation since we employed a transgenic HIVgp120 mouse model, which is known to closely recapitulate hallmarks of early HIV infection in brain and development of encephalitis. While this model provides valuable insights into the

Author Manuscript Author Manuscript Author Manuscript Author Manuscript

neurological effects of HIV during the initial stages, the findings observed in this system may not fully represent the experience of PWH who have mild HAND and are on effective ART. The majority of PWH access cART and experience milder forms of HAND. Future research in human cohorts in combination with additional new models are warranted to expand on the potential translational implications of our findings.

5. Conclusions

In summary, our findings show that endogenous IFNβ is important for normal memory dependent behavioral performance and modulates neuropathology in HIVgp120tg brains, indicating that its absence facilitates neurocognitive impairment and development of neuropathology. Moreover, in the absence of HIV, endogenous IFNβ appears to plays a vital role in maintaining neuronal homeostasis and memory function.

Supplementary Material

Refer to Web version on PubMed Central for supplementary material.

Acknowledgements

We thank Dr.Tomas Leanderson (Lund University, Lund, SE) for providing IFNβKO mice. We would also like thank Drs. Nina Yuan, Daniel Ojeda-Juárez, Deepika Bhullar and former lab assistant Rohan Shah for helping with the brain tissue harvest, Dr. Ana B. Sanchez for primer design, and the animal facility teams of the Sanford Burnham Prebys Medical Discovery Institute, The Scripps Research Institute, and the University of California Riverside, for assistance with the mouse colony.

Funding

This work was supported by funds form NIH, MH087332, MH104131, MH105330 and DA052209 to M.K. The sponsors have no role in study design, data collection or decision to submit the article for publications.

Availability of data or materials

The data generated during this study are available from the corresponding author upon reasonable request. The new mouse line will be shared through material transfer agreements (MTA).

Abbreviations

Actb	Actin Beta
ANOVA	Analysis of variance
BM	Barnes maze test
BSA	Bovine serum albumin
BCA	Bicinchoninic acid
BTN3A3	Butyrophilin subfamily 3 member A3
CNS	Central nervous system

Author Manuscript Author Manuscript Author Manuscript Author Manuscript

CREB1	cAMP responsive element binding protein 1
CD163	cluster of differentiation 163
DS	Dopamine serotonin
Gapdh	Glyceraldehyde-3-Phosphate Dehydrogenase
Gusb	Glucuronidase Beta
GFAP	Glial fibrillary acidic protein
GG	GABA Glutamate
GBP1	Guanylate binding protein 1
Hsp90ab1	Heat Shock Protein 90 Alpha Family Class B Member 1
HIVgp120tg	HIVgp120 transgenic mouse
HIV	Human immunodeficiency virus
HAND	HIV-associated neurocognitive disorder
IFN	Interferon
IFNβ	Interferon beta
IPA	Ingenuity Pathway Analysis
ISGs	Interferons stimulated genes
IFNβKO	IFNβ gene knockout
IFNAR	Interferon type 1 (IFN-α/β) receptor
Iba1	Ionized calcium-binding adaptor molecule 1
JNK	cJun N-terminal kinase
JAK-STAT	Janus kinase-signal transducer and activator of transcription
LCN2	Lipocalin
LDT	Light/dark transfer
LMA	Locomotor activity
MAPK	Mitogen-activated protein kinases
MAP-2	Microtubule-associated protein 2
NOR	Novel object recognition
OM	Optomotor

Author Manuscript Author Manuscript Author Manuscript Author Manuscript

PSMB8	Proteosome subunit beta type 8
PWH	People living with HIV
Syp	Synaptophysin
SIV	Simian immunodeficiency virus
STAT1	Signal transducer and activator of transcription 1
TSRI	The Scripps Research Institute's
WHO	World health organization
WT	Wild type

REFERENCES

Alammar L, Gama L, Clements JE, 2011. Simian Immunodeficiency Virus Infection in the Brain and Lung Leads to Differential Type I IFN Signaling during Acute Infection. The Journal of Immunology 186, 4008–4018. [PubMed: 21368232]

Barber SA, Herbst DS, Bullock BT, Gama L, Clements JE, 2004. Innate immune responses and control of acute simian immunodeficiency virus replication in the central nervous system. J Neurovirol 10 Suppl 1, 15–20. [PubMed: 14982734]

Bell JE, 2004. An update on the neuropathology of HIV in the HAART era. Histopathology 45, 549–559. [PubMed: 15569045]

Berg RK, Melchjorsen J, Rintahaka J, Diget E, Soby S, Horan KA, Gorelick RJ, Matikainen S, Larsen CS, Ostergaard L, Paludan SR, Mogensen TH, 2012. Genomic HIV RNA induces innate immune responses through RIG-I-dependent sensing of secondary-structured RNA. PLoS One 7, e29291. [PubMed: 22235281]

Borden EC, Sen GC, Uze G, Silverman RH, Ransohoff RM, Foster GR, Stark GR, 2007. Interferons at age 50: past, current and future impact on biomedicine. Nat Rev Drug Discov 6, 975–990. [PubMed: 18049472]

Cocchi F, DeVico AL, Garzino-Demo A, Arya SK, Gallo RC, Lusso P, 1995. Identification of RANTES, MIP-1 alpha, and MIP-1 beta as the major HIV-suppressive factors produced by CD8+ T cells. Science 270, 1811–1815. [PubMed: 8525373]

Doyle T, Goujon C, Malim MH, 2015. HIV-1 and interferons: who's interfering with whom? Nat Rev Microbiol 13, 403–413. [PubMed: 25915633]

Dziennis S, Alkayed NJ, 2008. Role of signal transducer and activator of transcription 3 in neuronal survival and regeneration. Rev Neurosci 19, 341–361. [PubMed: 19145989]

Erlandsson L, Blumenthal R, Eloranta ML, Engel H, Alm G, Weiss S, Leanderson T, 1998. Interferon-beta is required for interferon-alpha production in mouse fibroblasts. Curr Biol 8, 223–226. [PubMed: 9501984]

Gelman BB, Chen T, Lisinicchia JG, Soukup VM, Carmical JR, Starkey JM, Masliah E, Commins DL, Brandt D, Grant I, Singer EJ, Levine AJ, Miller J, Winkler JM, Fox HS, Luxon BA, Morgello S, National Neuro, A.T.C., 2012. The National NeuroAIDS Tissue Consortium brain gene array: two types of HIV-associated neurocognitive impairment. PLoS One 7, e46178. [PubMed: 23049970]

Hoefer MM, Sanchez AB, Maung R, de Rozieres CM, Catalan IC, Dowling CC, Thaney VE, Pina-Crespo J, Zhang D, Roberts AJ, Kaul M, 2015. Combination of methamphetamine and HIV-1 gp120 causes distinct long-term alterations of behavior, gene expression, and injury in the central nervous system. Exp Neurol 263, 221–234. [PubMed: 25246228]

Kaul M, Lipton SA, 1999. Chemokines and activated macrophages in HIV gp120-induced neuronal apoptosis. Proc Natl Acad Sci U S A 96, 8212–8216. [PubMed: 10393974]

Author Manuscript Author Manuscript Author Manuscript Author Manuscript

Kaul M, Zheng J, Okamoto S, Gendelman HE, Lipton SA, 2005. HIV-1 infection and AIDS: consequences for the central nervous system. Cell Death Differ 12 Suppl 1, 878–892. [PubMed: 15832177]

Kim EK, Choi EJ, 2010. Pathological roles of MAPK signaling pathways in human diseases. Biochim Biophys Acta 1802, 396–405. [PubMed: 20079433]

Kitai R, Zhao ML, Zhang N, Hua LL, Lee SC, 2000. Role of MIP-1beta and RANTES in HIV-1 infection of microglia: inhibition of infection and induction by IFNbeta. J Neuroimmunol 110, 230–239. [PubMed: 11024554]

Koga Y, Tsurumaki H, Aoki-Saito H, Sato M, Yatomi M, Takehara K, Hisada T, 2019. Roles of Cyclic AMP Response Element Binding Activation in the ERK1/2 and p38 MAPK Signalling Pathway in Central Nervous System, Cardiovascular System, Osteoclast Differentiation and Mucin and Cytokine Production. Int J Mol Sci 20.

Krivine A, Force G, Servan J, Cabee A, Rozenberg F, Dighiero L, Marguet F, Lebon P, 1999. Measuring HIV-1 RNA and interferon-alpha in the cerebrospinal fluid of AIDS patients: insights into the pathogenesis of AIDS Dementia Complex. J Neurovirol 5, 500–506. [PubMed: 10568887]

Le Dreau G, Calament G, Volant A, Savary O, Cauvin JM, Robaszkiewicz M, Gouerou H, 1998. [Diagnosis of mediastinal neuro-endocrine tumor using endosonography guided transesophageal puncture biopsy]. Gastroenterol Clin Biol 22, 87–90. [PubMed: 9762170]

Lee S, Lee DK, 2018. What is the proper way to apply the multiple comparison test? Korean J Anesthesiol 71, 353–360. [PubMed: 30157585]

Li T, Zhao X, Duan J, Cui S, Zhu K, Wan Y, Liu S, Peng Z, Wang L, 2021. Targeted inhibition of STAT3 in neural stem cells promotes neuronal differentiation and functional recovery in rats with spinal cord injury. Exp Ther Med 22, 711. [PubMed: 34007320]

Livak KJ, Schmittgen TD, 2001. Analysis of Relative Gene Expression Data Using Real-Time Quantitative PCR and the 2−ΔΔCT Method. Methods 25, 402–408. [PubMed: 11846609]

Maung R, Hoefer MM, Sanchez AB, Sejbuk NE, Medders KE, Desai MK, Catalan IC, Dowling CC, de Rozieres CM, Garden GA, Russo R, Roberts AJ, Williams R, Kaul M, 2014. CCR5 knockout prevents neuronal injury and behavioral impairment induced in a transgenic mouse model by a CXCR4-using HIV-1 glycoprotein 120. J Immunol 193, 1895–1910. [PubMed: 25031461]

Medders KE, Sejbuk NE, Maung R, Desai MK, Kaul M, 2010. Activation of p38 MAPK is required in monocytic and neuronal cells for HIV glycoprotein 120-induced neurotoxicity. J Immunol 185, 4883–4895. [PubMed: 20855878]

Minagawa T, Mizuno K, Hirano S, Asano M, Numata A, Kohanawa M, Nakane A, Hachimori K, Tamagawa S, Negishi M, et al. , 1989. Detection of high levels of immunoreactive human beta-1 interferon in sera from HIV-infected patients. Life Sci 45, iii–vii.

Mocchetti I, Bachis A, 2004. Brain-derived neurotrophic factor activation of TrkB protects neurons from HIV-1/gp120-induced cell death. Crit Rev Neurobiol 16, 51–57. [PubMed: 15581399]

Mumby DG, Tremblay A, Lecluse V, Lehmann H, 2005. Hippocampal damage and anterograde object-recognition in rats after long retention intervals. Hippocampus 15, 1050–1056. [PubMed: 16145694]

Ojeda-Juarez D, Shah R, Fields JA, Harahap-Carrillo IS, Koury J, Maung R, Gelman BB, Baaten BJ, Roberts AJ, Kaul M, 2020. Lipocalin-2 mediates HIV-1 induced neuronal injury and behavioral deficits by overriding CCR5-dependent protection. Brain Behav Immun 89, 184–199. [PubMed: 32534984]

Paylor R, Zhao Y, Libbey M, Westphal H, Crawley JN, 2001. Learning impairments and motor dysfunctions in adult Lhx5-deficient mice displaying hippocampal disorganization. Physiol Behav 73, 781–792. [PubMed: 11566211]

Perrella O, Carreiri PB, Perrella A, Sbreglia C, Gorga F, Guarnaccia D, Tarantino G, 2001. Transforming growth factor beta-1 and interferon-alpha in the AIDS dementia complex (ADC): possible relationship with cerebral viral load? Eur Cytokine Netw 12, 51–55. [PubMed: 11282546]

Rho MB, Wesselingh S, Glass JD, McArthur JC, Choi S, Griffin J, Tyor WR, 1995. A potential role for interferon-alpha in the pathogenesis of HIV-associated dementia. Brain Behav Immun 9, 366–377. [PubMed: 8903853]

Author Manuscript Author Manuscript Author Manuscript Author Manuscript

Ru W, Tang SJ, 2017. HIV-associated synaptic degeneration. Molecular brain 10, 40. [PubMed: 28851400]

Sanders VJ, Pittman CA, White MG, Wang G, Wiley CA, Achim CL, 1998. Chemokines and receptors in HIV encephalitis. AIDS 12, 1021–1026. [PubMed: 9662198]

Sanna PP, Repunte-Canonigo V, Masliah E, Lefebvre C, 2017. Gene expression patterns associated with neurological disease in human HIV infection. PLoS One 12, e0175316. [PubMed: 28445538]

Saylor D, Dickens AM, Sacktor N, Haughey N, Slusher B, Pletnikov M, Mankowski JL, Brown A, Volsky DJ, McArthur JC, 2016. HIV-associated neurocognitive disorder--pathogenesis and prospects for treatment. Nat Rev Neurol 12, 234–248. [PubMed: 26965674]

Schoggins JW, Wilson SJ, Panis M, Murphy MY, Jones CT, Bieniasz P, Rice CM, 2011. A diverse range of gene products are effectors of the type I interferon antiviral response. Nature 472, 481–485. [PubMed: 21478870]

Singh H, Koury J, Kaul M, 2021. Innate Immune Sensing of Viruses and Its Consequences for the Central Nervous System. Viruses 13.

Singh H, Ojeda-Juárez D, Maung R, Shah R, Roberts AJ, Kaul M, 2020. A pivotal role for Interferon-α receptor-1 in neuronal injury induced by HIV-1. Journal of Neuroinflammation 17, 226. [PubMed: 32727588]

Thaney VE, Kaul M, 2019. Type I Interferons in NeuroHIV. Viral Immunol 32, 7–14. [PubMed: 30260742]

Thaney VE, O'Neill AM, Hoefer MM, Maung R, Sanchez AB, Kaul M, 2017. IFNbeta Protects Neurons from Damage in a Murine Model of HIV-1 Associated Brain Injury. Sci Rep 7, 46514. [PubMed: 28425451]

Toggas SM, Masliah E, Rockenstein EM, Rall GF, Abraham CR, Mucke L, 1994. Central nervous system damage produced by expression of the HIV-1 coat protein gp120 in transgenic mice. Nature 367, 188–193. [PubMed: 8114918]

Winters BD, Forwood SE, Cowell RA, Saksida LM, Bussey TJ, 2004. Double dissociation between the effects of peri-postrhinal cortex and hippocampal lesions on tests of object recognition and spatial memory: heterogeneity of function within the temporal lobe. J Neurosci 24, 5901–5908. [PubMed: 15229237]

Yang B, Akhter S, Chaudhuri A, Kanmogne GD, 2009. HIV-1 gp120 induces cytokine expression, leukocyte adhesion, and transmigration across the blood-brain barrier: modulatory effects of STAT1 signaling. Microvasc Res 77, 212–219. [PubMed: 19103208]

Author Manuscript Author Manuscript Author Manuscript Author Manuscript

Highlights

1. Genetic ablation of IFNβ modulates HIVgp120-induced neuropathology in a sex-dependent fashion
2. Endogenous IFNβ is required for normal function of spatial and recognition memory
3. Genetic ablation of IFNβ aggravates impairment of spatial memory in the presence of HIVgp120
4. Endogenous IFNβ regulates expression of neuroinflammatory factors induced during exposure to HIVgp120
5. Genetic ablation of IFNβ alters expression of neurotransmission-related genes in a sex-dependent fashion

Author Manuscript Author Manuscript Author Manuscript Author Manuscript

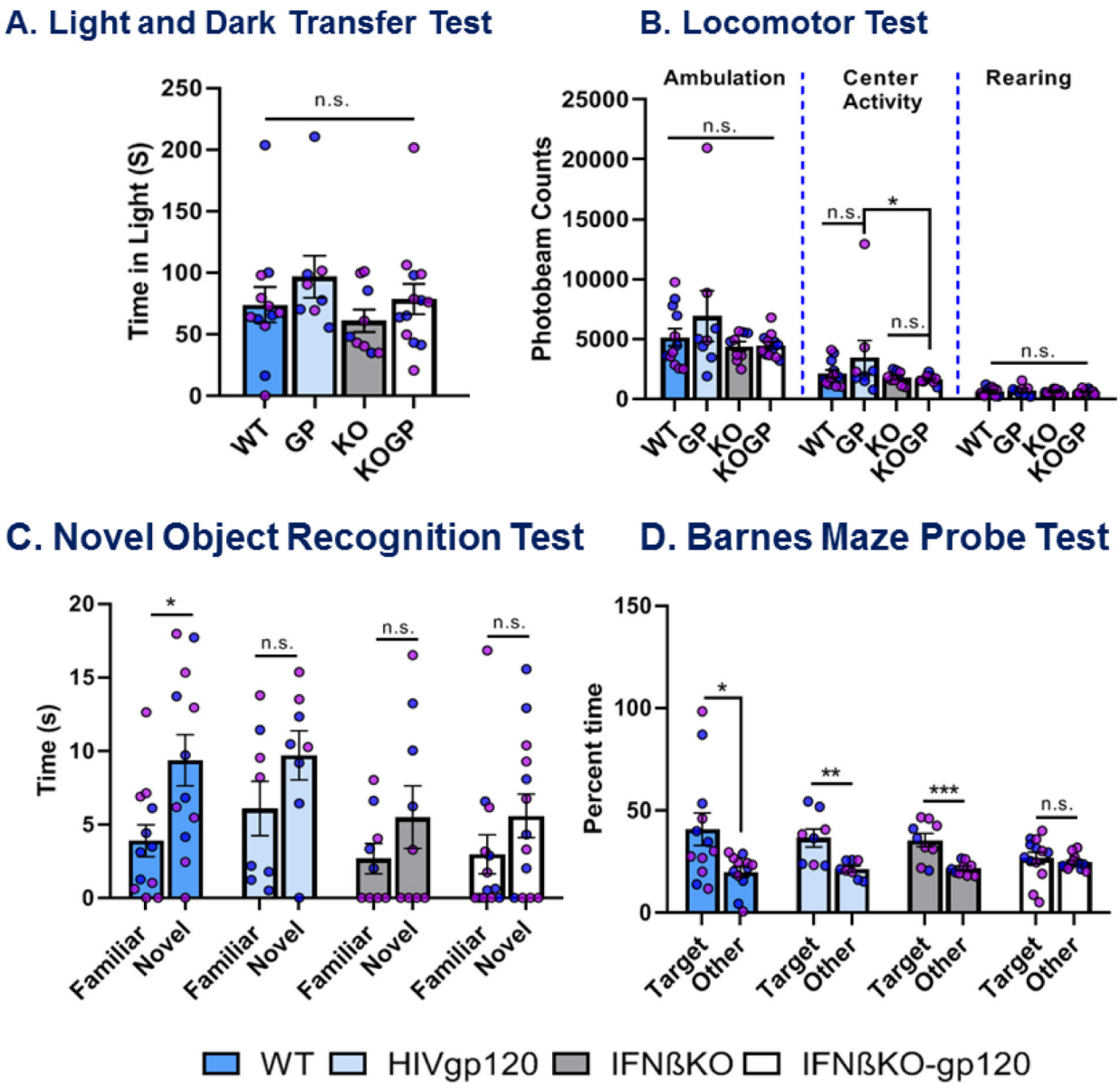

Fig. 1. IFNβ affects recognition and spatial memory.

Nine to 10 month-old mice, WT (male:5; female:7), HIVgp120/GP (male:5; female:3), IFNβKO/KO (male:3; female:6) and IFNβKO-HIVgp120/KOGP (male:6; female:7) were behaviorally assessed as described in Materials and Methods. **(A)** Light/dark transfer test for anxiety like behavior. **(B)** Locomotor test showing ambulation, center activity and rearing. **(C)** Novel object recognition for recognition memory. **(D)** Barnes Maze probe test for spatial learning and memory. All data are represented as means ± SEM. Statistical analysis was performed as described in the methods section. *** $P < 0.001$, ** $P < 0.01$, * $P \leq 0.05$; ANOVAs and post hoc tests; n = 8–13 (females [pink dots] and males [blue dots]) per group/genotype; n.s., not significant.

Author Manuscript Author Manuscript Author Manuscript Author Manuscript

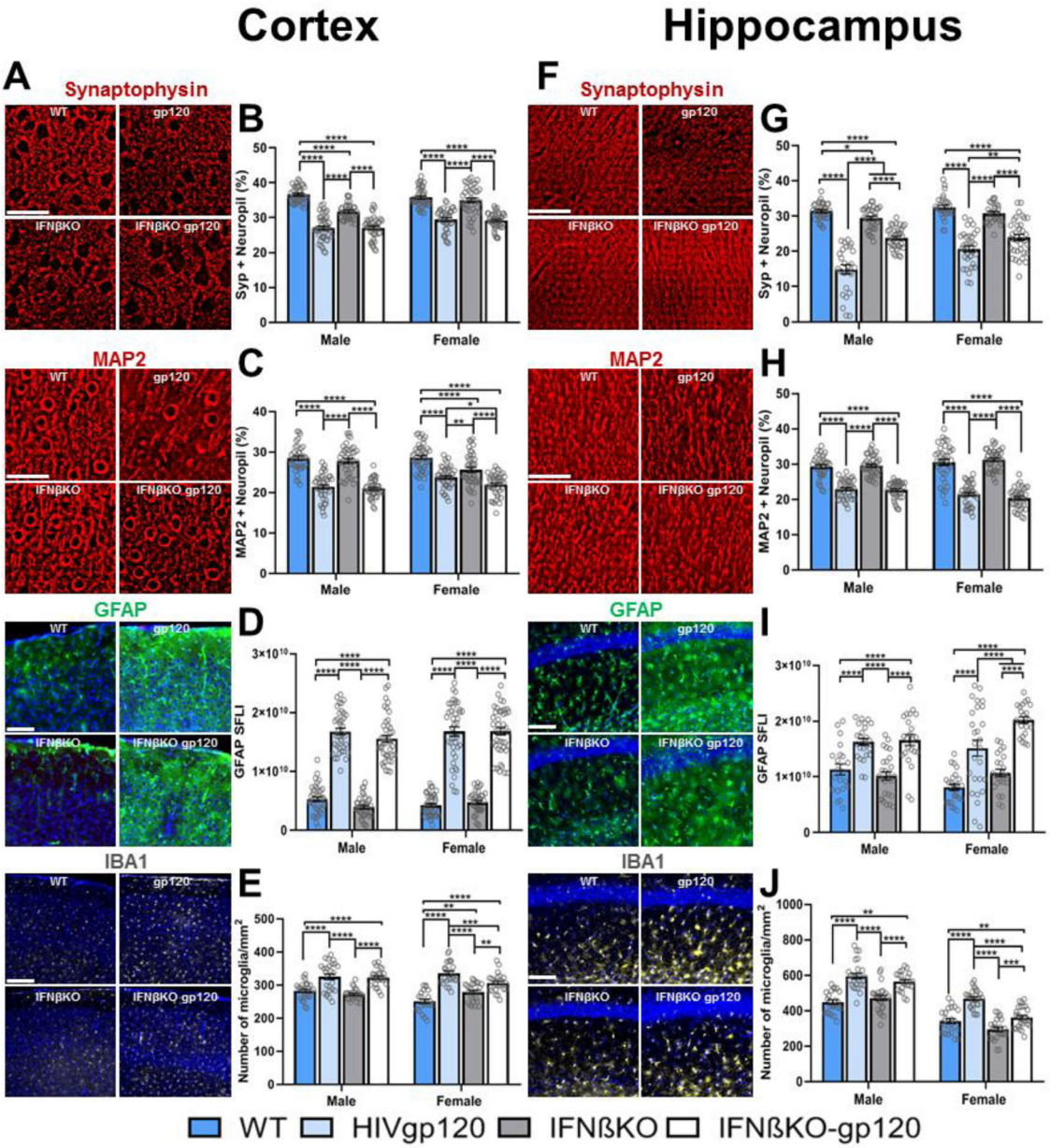

Fig. 2. Effect of IFNβ deficiency on presynaptic terminals, neuronal dendrites, astrocytosis and microgliosis.

Brains of 9–10 months old mice were histologically analyzed as described in the methods. **(A & F)** Representative images of cortex (layer 3) and hippocampus (CA1) immunolabeled for neuronal synaptophysin (SYP) and MAP-2 (deconvolution microscopy; scale bar = 40 μm), astrocytic GFAP and Iba1 microglia (florescence microscopy; scale bar = 200 μm). **(B&G)** Quantification of neuropil positive for synaptophysin, **(C & H)** neuronal MAP-2, **(D & I)** fluorescence signal for astrocytic GFAP. **(E & J)** Counts for Iba1+ microglia. Genotypes: WT, HIVgp120 (GP), IFNβKO (KO), and IFNβKO-HIVgp120 (KOGP).Values are means ± SEM; **** $P < 0.0001$, *** $P < 0.001$, ** $P < 0.01$, * $P < 0.05$; ANOVA and Fisher's PLSD post hoc test; n = 6 animals (3 males and 3 females) per group/genotype.

Author Manuscript
Author Manuscript
Author Manuscript
Author Manuscript

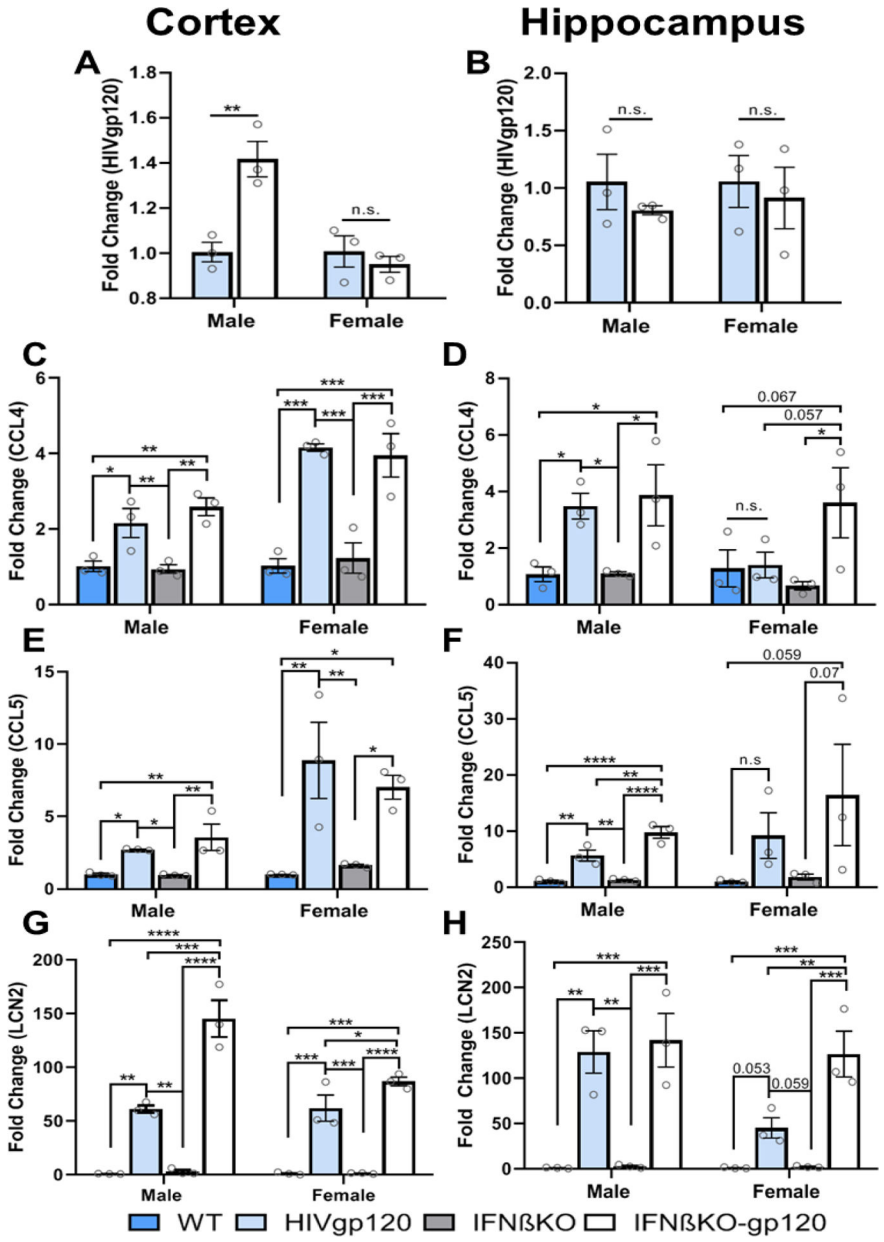

Fig. 3. Sex-dependent effects of IFNβ deficiency on RNA expression of transgenic viral HIVgp120 and host genes.

The mRNA expression in the cortex and hippocampus of 9–10 months-old mice, were detected by quantitative RT-PCR as described in material and method section. (A & B) HIVgp120; (C & D) CCL4; (E & F) CCL5 and (G &H) LCN2. The obtained CT values were normalized to the level of GAPDH mRNA. Values are means ± SEM; **** $P < 0.0001$, *** $P < 0.001$, ** $P < 0.01$, * $P < 0.05$; ANOVA and Fisher's PLSD post hoc test; n = 3 mice per group/genotype; n.s., not significant.

Author Manuscript Author Manuscript Author Manuscript Author Manuscript

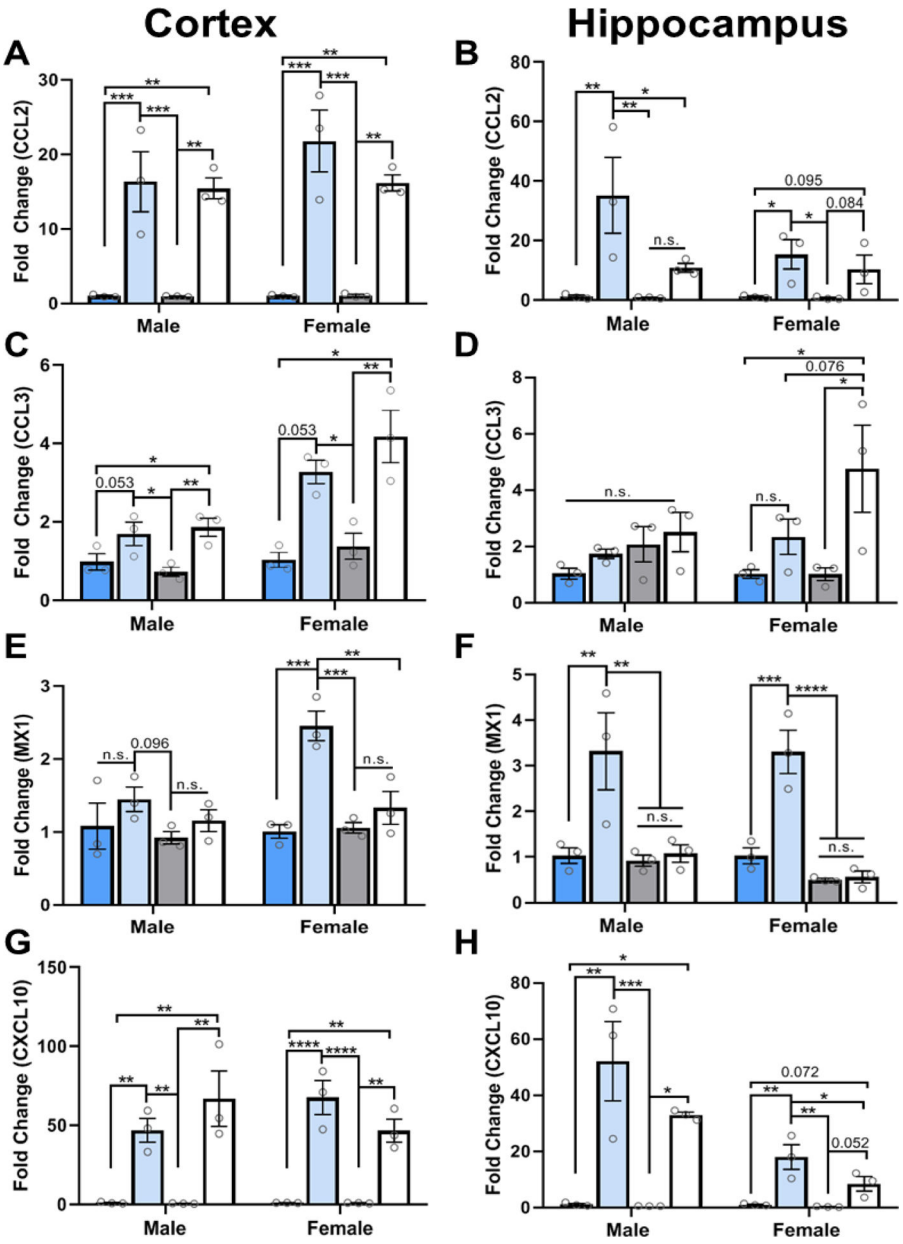

Author Manuscript Author Manuscript Author Manuscript Author Manuscript

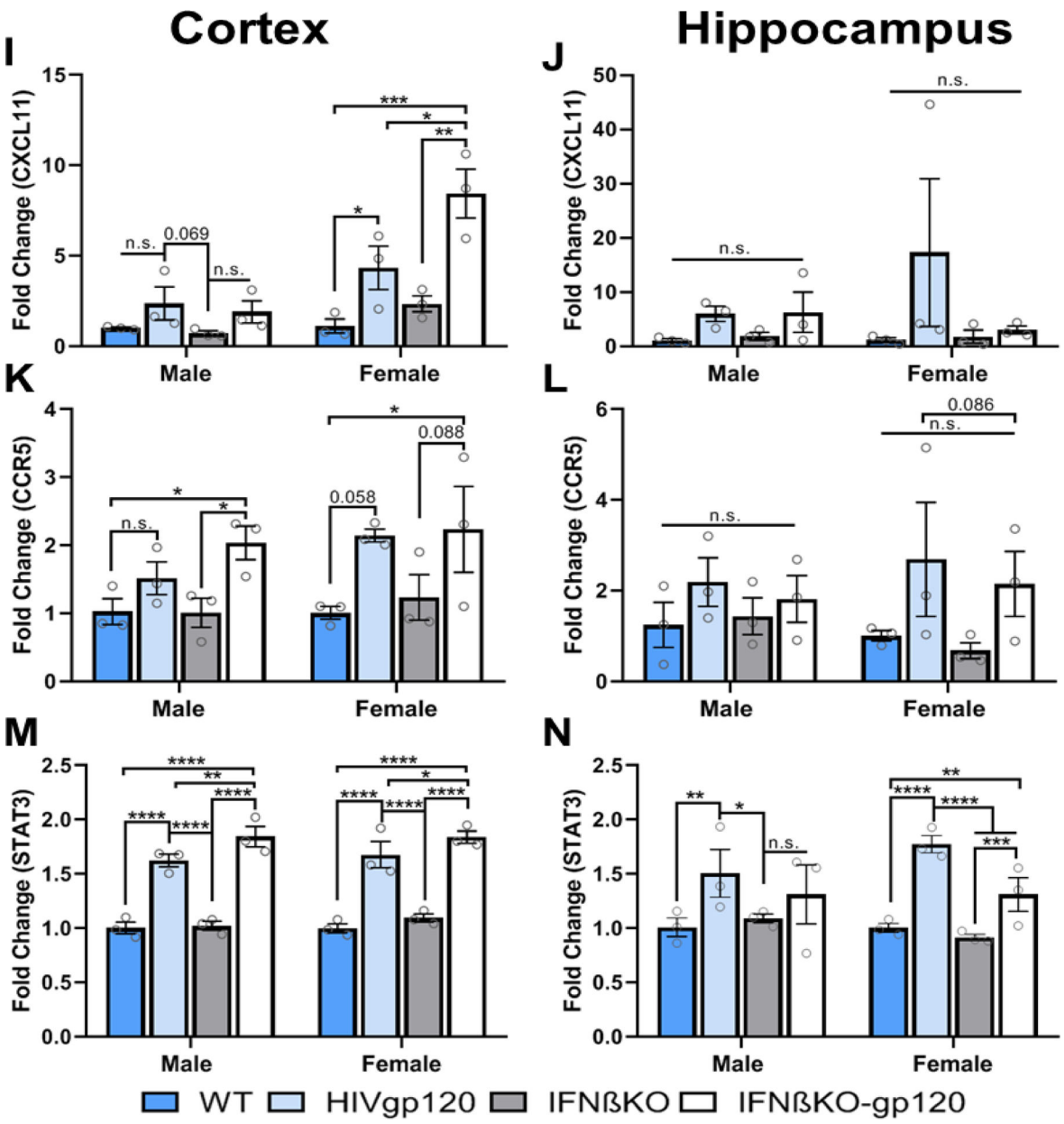

Fig. 4. (Previous and this page) Effects of IFNβ deficiency on RNA expression of host genes.

The mRNA expression in the cortex and hippocampus of 9–10 months-old mice, were detected by quantitative RT-PCR as described in material and method section. **(A & B)** CCL2; **(C & D)** CCL3; **(E & F)** MX1; **(G & H)** CXCL10; **(I & J)** CXCL11; **(K & L)** CCR5 and **(M & N)** STAT3. The obtained CT values were normalized to the level of GAPDH mRNA. Values are means ± SEM; **** $P < 0.0001$, *** $P < 0.001$, ** $P < 0.01$, * $P < 0.05$; ANOVA and Fisher's PLSD post hoc test; n = 3 mice per group/genotype/sex; n.s., not significant.

Author Manuscript Author Manuscript Author Manuscript Author Manuscript

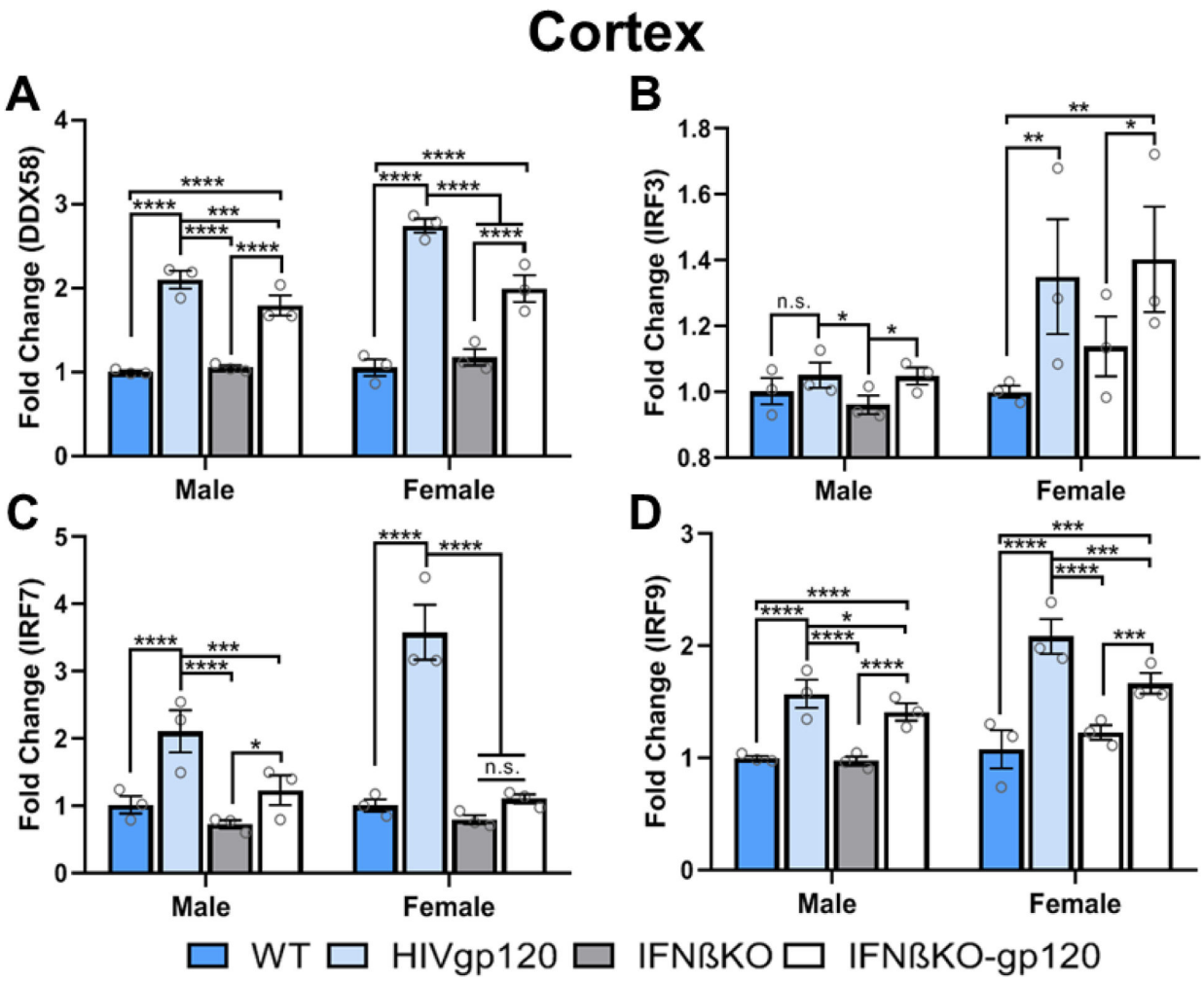

Fig. 5. Effects of IFNβ deficiency on RNA expression of DDX58, IRF3, IRF7 and IRF9.

The mRNA expression levels of DDX58 **(A)**, IRF3 **(B)**, IRF7 **(C)**, and IRF9 **(D)** were measured in the cortex of 9–10-month-old mice using quantitative RT-PCR. The obtained CT values were then normalized to the level of GAPDH mRNA. The values are presented as means ± SEM; **** $P < 0.0001$, *** $P < 0.001$, ** $P < 0.01$, * $P < 0.05$; ANOVA and Fisher's PLSD post hoc test; n = 3 mice per group/genotype/sex; n.s., not significant.

Author Manuscript Author Manuscript Author Manuscript Author Manuscript

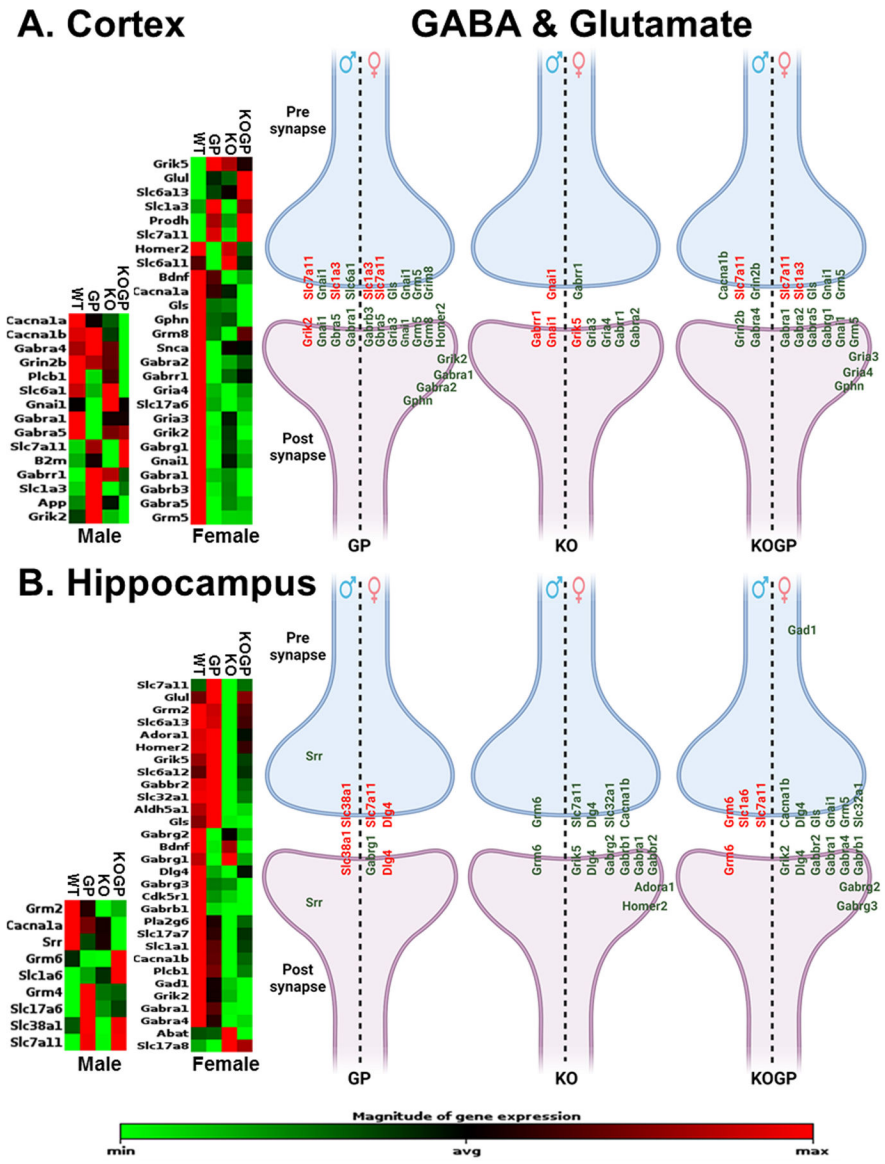

Fig. 6. (Previous page) Differential gene expression associated with GABA and glutamate neurotransmission systems in the cortex and hippocampus.

Clustergram heat map of mRNA expression of the GABA/Glutamate system in the cortex **(A)** and in the hippocampus **(B)** showing gene expression profile of WT, HIVgp120, and IFNβ-deficient mice with or without HIVgp120. Red indicate higher gene expression while green indicates the lower expression in the sample set normalized by rows. RNA was analyzed using RT^2 Profiler PCR Array and the associated Qiagen data analysis software. The heat maps represent significantly changed genes as the averages of three biological replicates. The figure on the right is a schematic representation of the pre- and post-synaptic distribution of differentially expressed genes in neurons of each genotype. Genotypes: WT, HIVgp120 (GP), IFNβKO (KO), and IFNβKO-HIVgp120 (KOGP).

Author Manuscript Author Manuscript Author Manuscript Author Manuscript

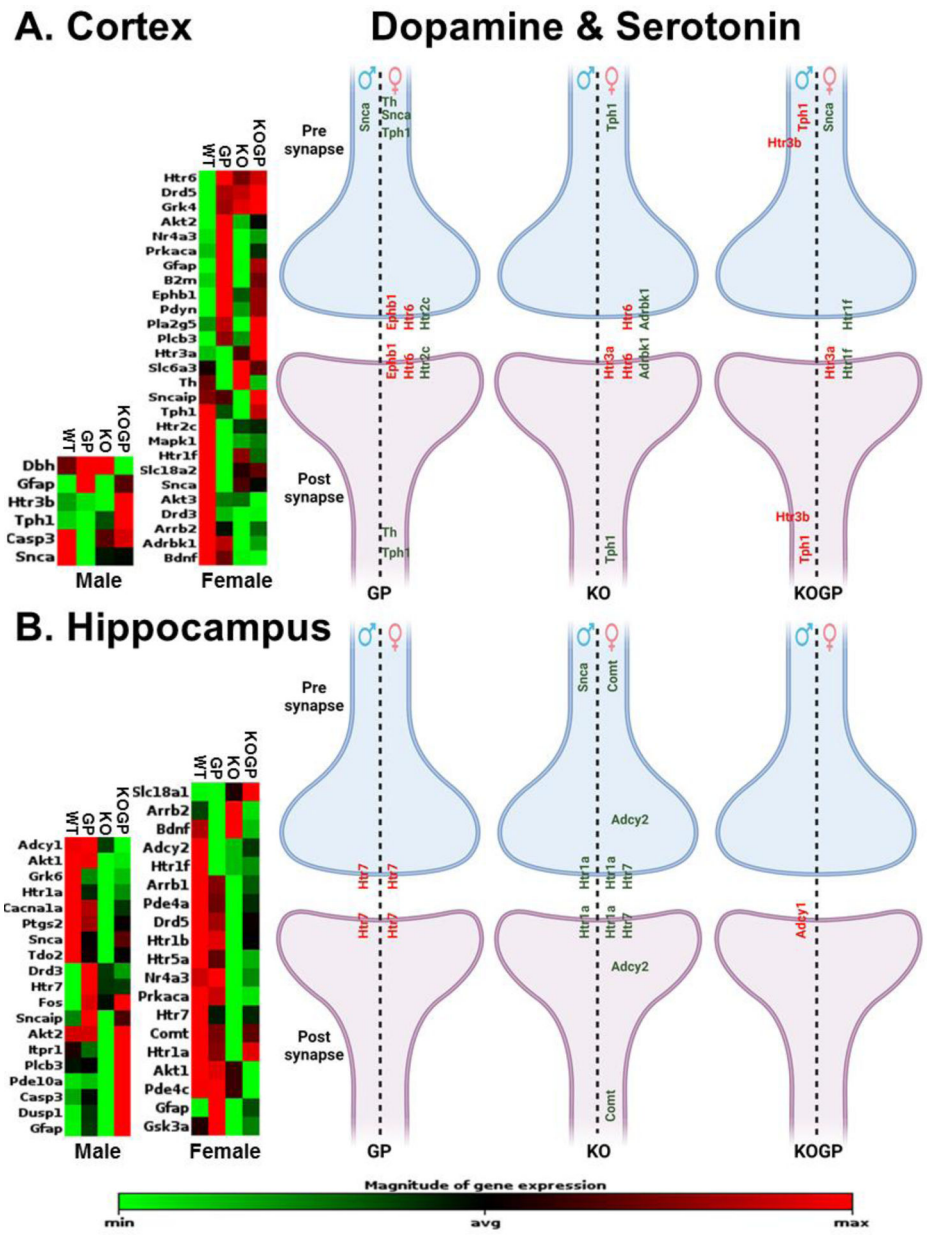

Fig. 7. (Previous page) Differential gene expression associated with dopamine serotonin neurotransmission systems in the cortex and hippocampus.

Clustergram heat map of dopamine/serotonin systems in the cortex **(A)** and in the hippocampus **(B)** showing gene expression profile of WT, HIVgp120-transgenic, IFNβ-deficient mice with or without HIVgp120. Red indicates the higher gene expression while green indicate the lower gene expression in the sample set. RNA was analyzed using RT^2 Profiler PCR Array and the associated Qiagen data analysis software. The heat maps represent significantly changed genes as the averages of three biological replicates. The figure on the right is a schematic representation of the pre- and post-synaptic distribution of differentially expressed genes in neurons of each genotype. Genotypes: WT, HIVgp120 (GP), IFNβKO (KO), and IFNβKO-HIVgp120 (KOGP).

Author Manuscript Author Manuscript Author Manuscript Author Manuscript

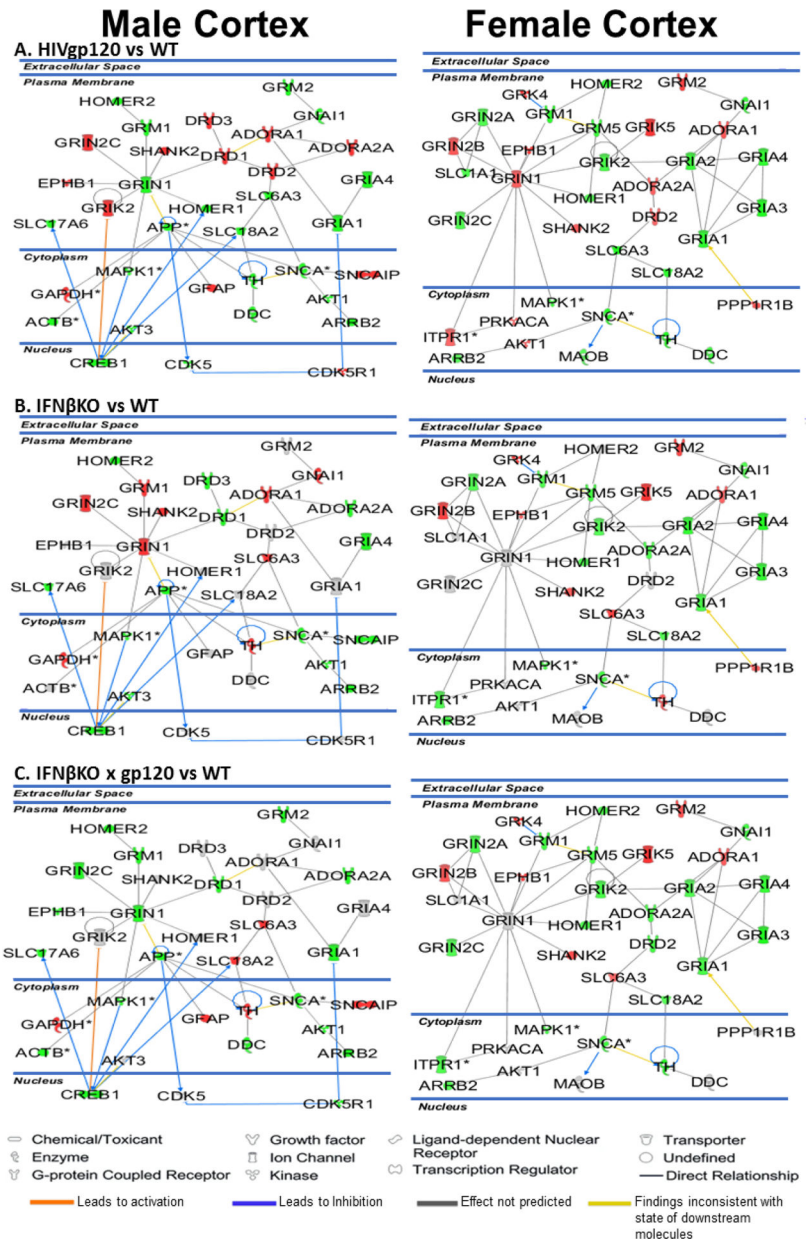

Fig. 8. (Previous page) Functional neural gene networks of neurotransmission affected by HIVgp120 and IFNβ deficiency in the cortex.

RNA expression data obtained with the GABA/glutamate RT^2 Profiler PCR Array were analyzed using IPA software. **(A)** HIVgp120 versus WT, **(B)** IFNβKO versus WT, **(C)** IFNβKO-HIVgp120 versus WT. Green indicates down-regulated while red reflects up-regulated genes respectively. The components without color represent genes were include by IPA without experimentally determined expression levels. IPA identified for each sex a different highest scoring gene direct interaction network in which alterations on expression levels were driven by HIVgp120 in the absence or presence of IFNβ. * Indicates genes for which differential regulation reached significance in the RT^2 Profiler PCR Array (* $P < 0.05$; modified t-test).

Author Manuscript Author Manuscript Author Manuscript Author Manuscript

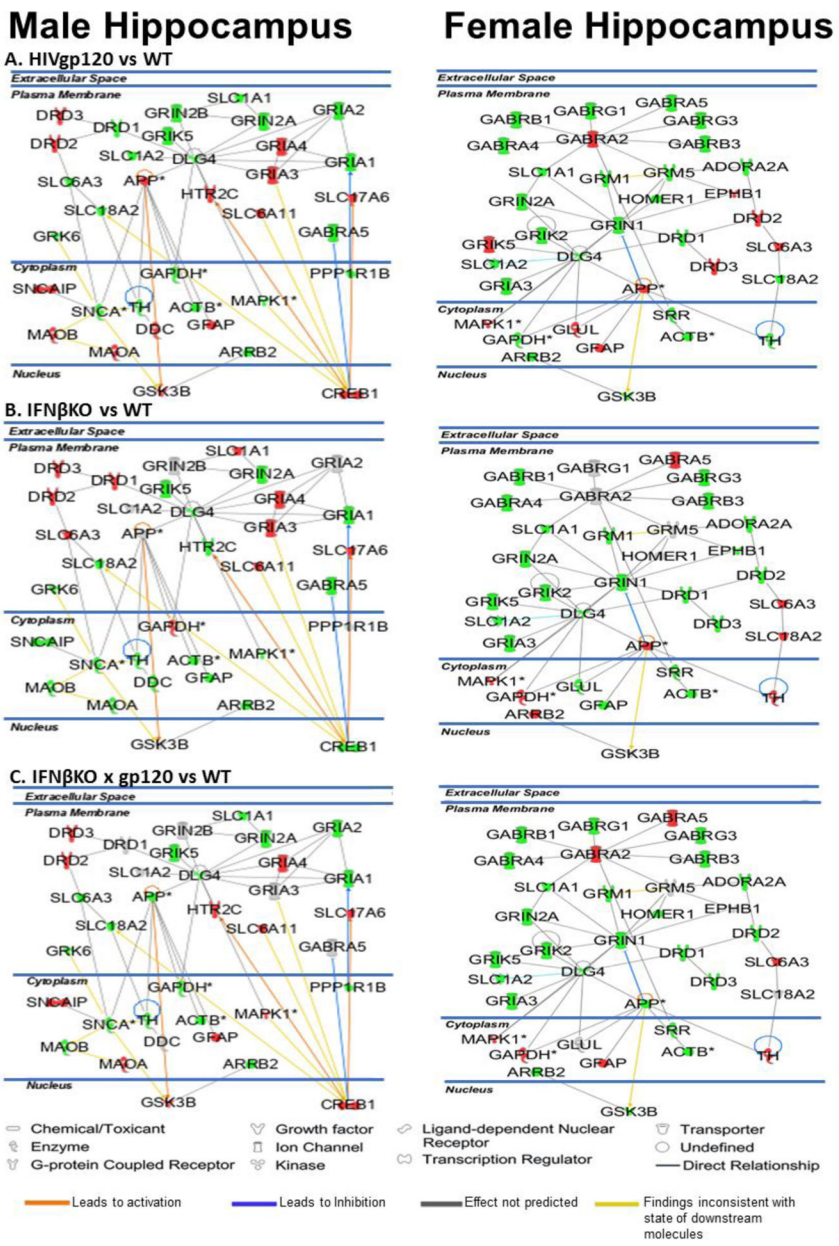

Fig. 9. (Next page) Functional neural gene networks of neurotransmission affected by HIVgp120 and IFNβ deficiency in the hippocampus.

RNA expression data obtained with the dopamine/serotonin RT^2 Profiler PCR Array were analyzed using IPA software. **(A)** HIVgp120 versus WT, **(B)** IFNβKO versus WT, **(C)** IFNβKO-HIVgp120 versus WT. Green indicates down-regulated while red reflects up-regulated genes respectively. Components without color represent genes without experimentally determined expression levels. IPA identified for each sex a different highest scoring gene network in which alterations on expression levels were driven by HIVgp120 in the absence or presence of IFNβ. * Indicates genes for which differential regulation reached significance in the RT^2 Profiler PCR Array (* $P < 0.05$; modified t-test).

Author Manuscript Author Manuscript Author Manuscript Author Manuscript

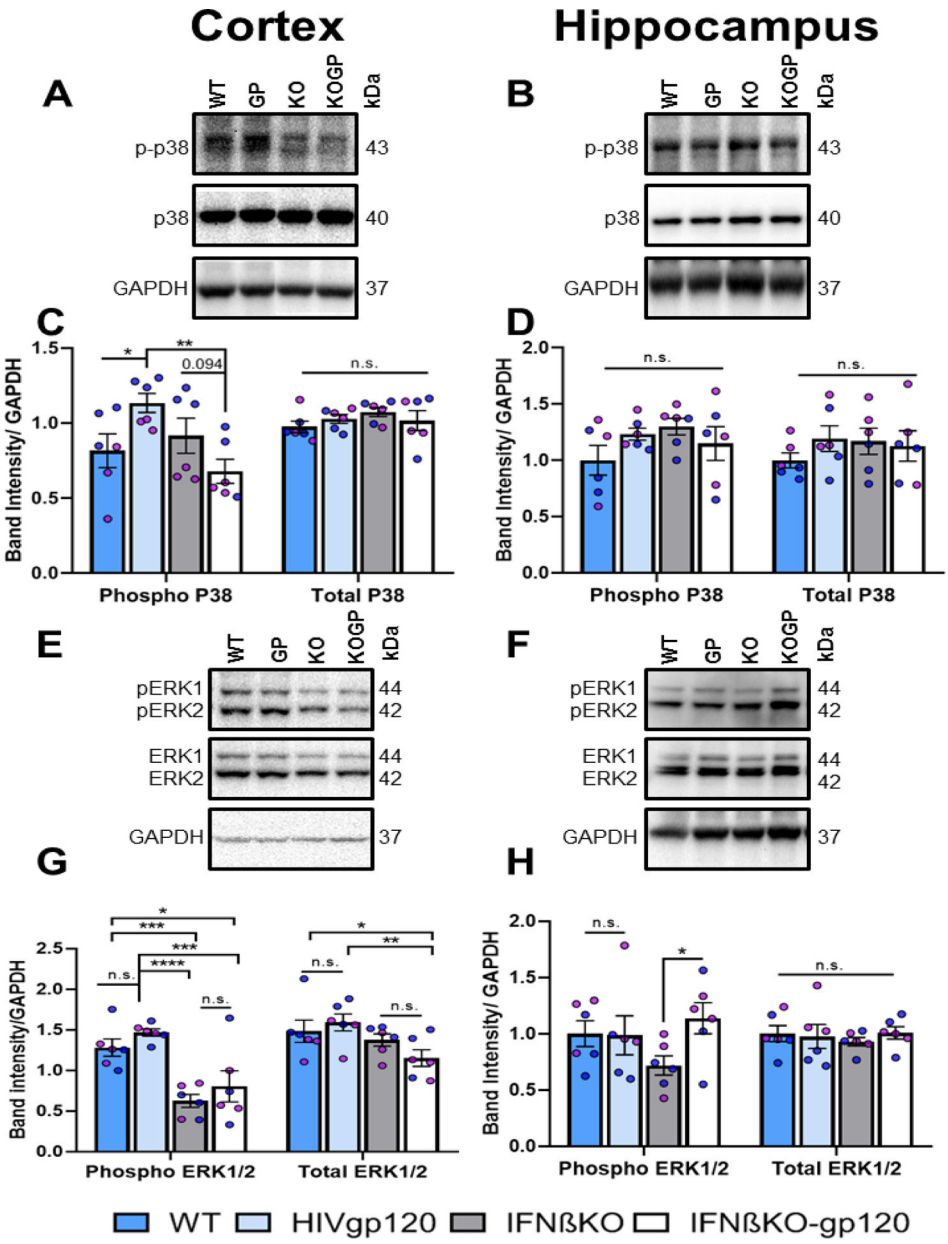

Fig. 10. The effect of HIVgp120 and IFNβ deficiency on the phosphorylation levels of p38 MAPK and ERK1/2.

The phosphorylation level of p38 and ERK1/2 in the cortex and hippocampus were measured using Western blotting. Representative Western blot of phospho p38(p-p38), p38 protein, and GAPDH in cortex **(A)** and hippocampus **(B)**. The graph shows quantification of p-p38 and p38 by densitometry using normalization to GAPDH in the cortex **(C)** and hippocampus **(D)**. Representative Western blot of phospho-ERK1/2 (pERK1/2), ERK1/2 total protein, and GAPDH in cortex **(E)** and hippocampus **(F)**. The graph shows densitometry analysis of pERK1/2 and ERK1/2 normalized to GAPDH in the cortex **(G)** and hippocampus **(H)**. Values are means ± SEM; **** $P < 0.0001$, *** $P < 0.001$, ** $P < 0.01$, * $P < 0.05$; ANOVA and Fisher's PLSD post hoc test; n = 6 animals (3 males and 3 females) 9–10 months-old animals per group/genotype; females [pink dots] and males [blue

dots]; n.s., not significant). Genotypes: Wildtype (WT), HIVgp120tg (GP), IFNβKO (KO), and IFNβKO × HIVgp120 (KOGP).

Author Manuscript Author Manuscript Author Manuscript Author Manuscript

Author Manuscript Author Manuscript Author Manuscript Author Manuscript

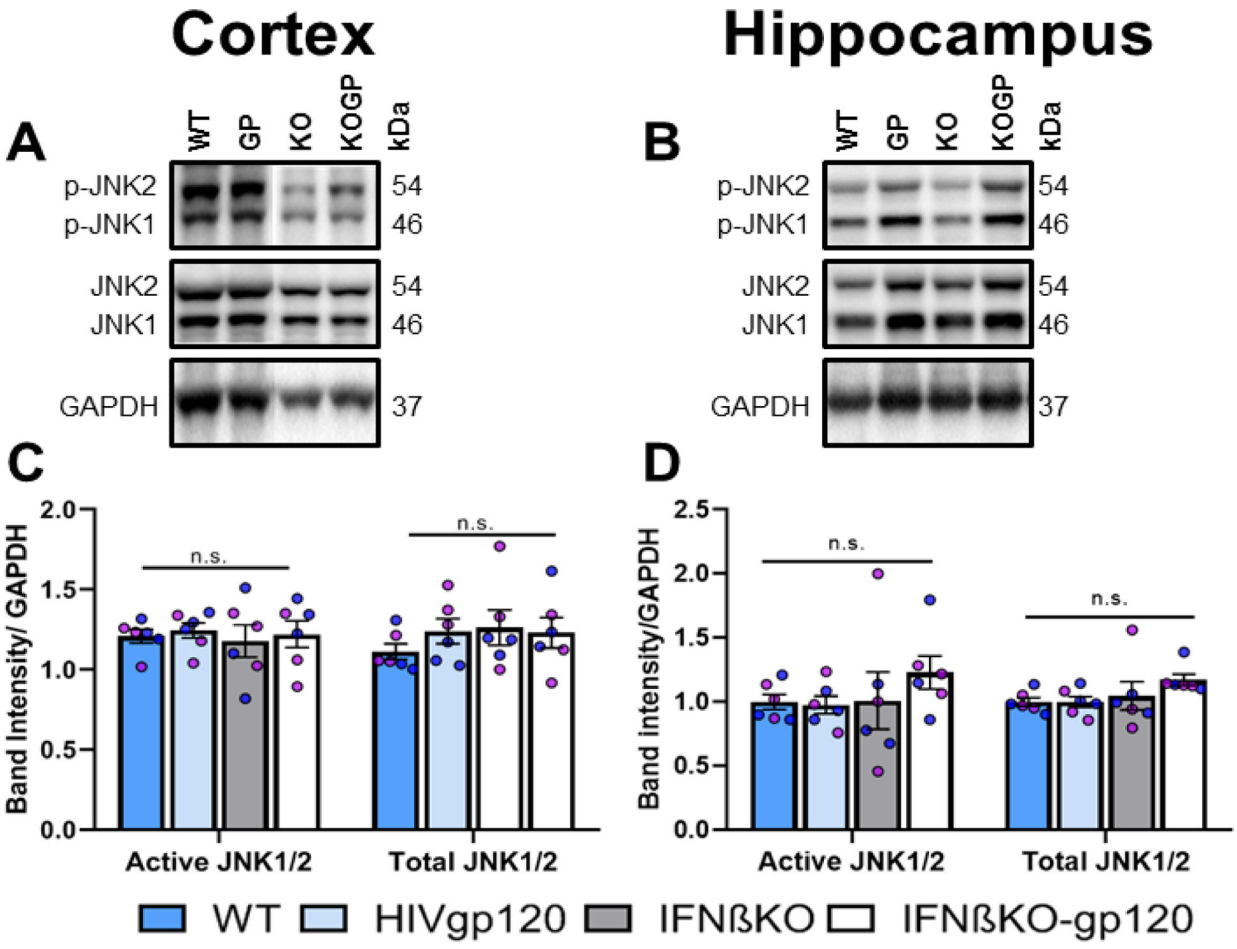

Fig. 11. IFNβ deficiency does not alter the expression of JNK in cortex and hippocampus of HIVgp120 mice.

The protein expression of phospho-JNK1/2 and JNK1/2 were assessed using immunoblotting. Representative western blot images and densitometry analysis of p-JNK1/2 and JNK1/2 normalized to GAPDH in the cortex (**A** and **C**) and hippocampus (**B** and **D**). Genotypes: WT (WT), HIVgp120tg (GP), IFNβKO (KO) and IFNβKO x HIVgp120 (KOGP). Values are means ± SEM; ANOVA and Fisher's PLSD post hoc test; n = 6 animals (3 males and 3 females) 9–10 months-old animals per group/genotype; females [pink dots] and males [blue dots]; n.s., not significant). Genotypes: Wildtype (WT), HIVgp120tg (GP), IFNβKO (KO), and IFNβKO × HIVgp120 (KOGP).

Author Manuscript Author Manuscript Author Manuscript Author Manuscript

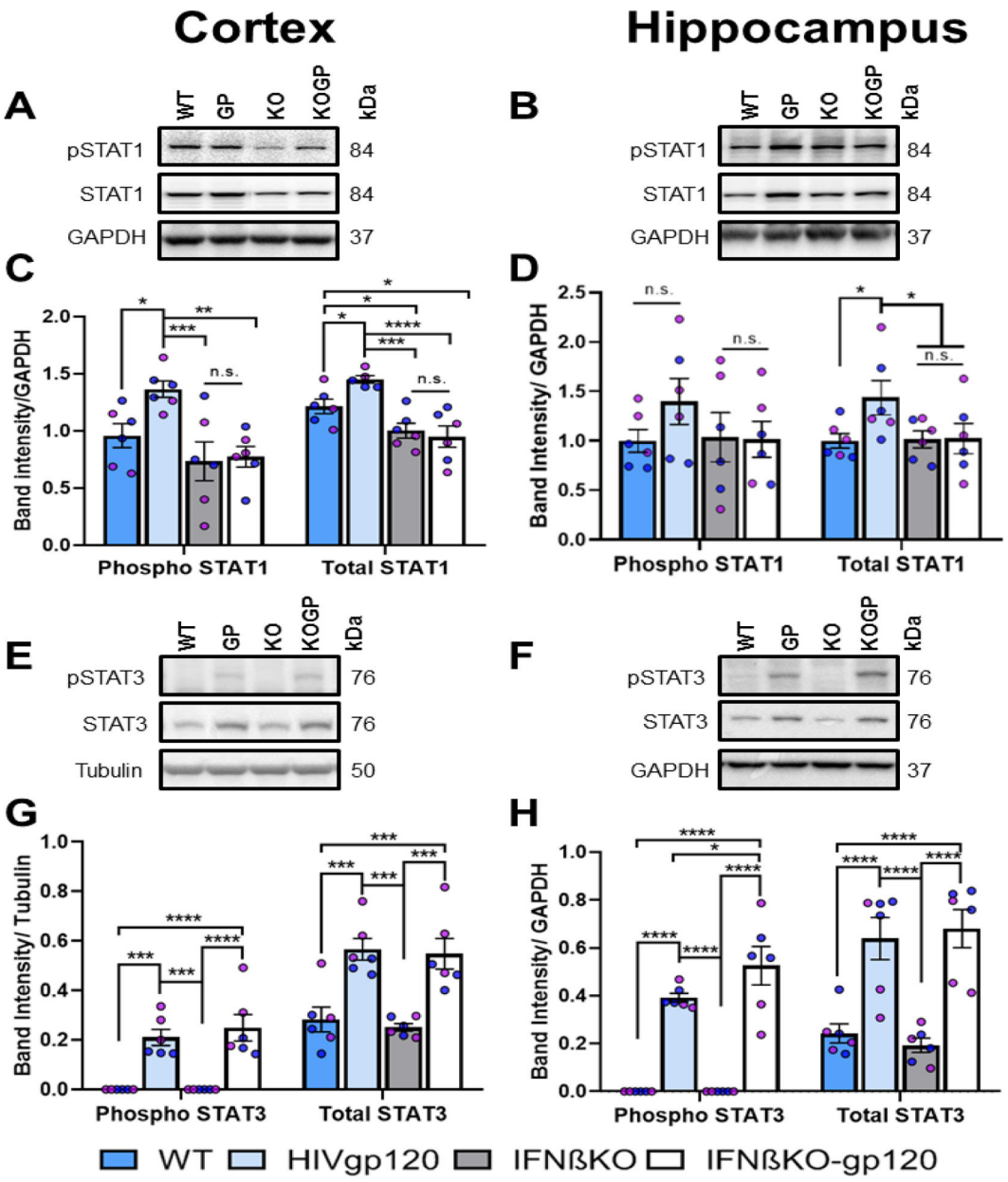

Fig. 12. The effect of HIVgp120 and IFNβ deficiency on the phosphorylation levels of STAT1 and STAT3.

The phosphorylation level of STAT1 and STAT3 in the cortex and hippocampus were measured using Western blotting. Representative Western blot of pSTAT1, STAT1, and GAPDH in cortex **(A)** and hippocampus **(B)**. The graph shows quantification of pSTAT1 and STAT1 by densitometry using normalization to GAPDH in the cortex **(C)** and hippocampus **(D)**. Representative Western blot of pSTAT3, STAT3, and tubulin in cortex (**E**) and hippocampus (**F**). The graph shows densitometry analysis of pSTAT3 and STAT3 normalized to tubulin in the cortex (**G**) and hippocampus (**H**). Values are means ± SEM; **** $P < 0.0001$, *** $P < 0.001$, ** $P < 0.01$, * $P < 0.05$; ANOVA and Fisher's PLSD post hoc test; n = 6 animals (3 males and 3 females) 9–10 months-old animals per group/

genotype; females [pink dots] and males [blue dots]; n.s., not significant). Genotypes: WT, HIVgp120 (GP), IFNβKO (KO), and IFNβKO-HIVgp120 (KOGP).

Author Manuscript Author Manuscript Author Manuscript Author Manuscript